PERSPECTIVES

Differential Occupancy of Somatodendritic and Postsynaptic $5HT_{1A}$ Receptors by Pindolol: A Dose-Occupancy Study with [^{11}C]WAY 100635 and Positron Emission Tomography in Humans

Diana Martinez, M.D., Dah-Ren Hwang, Ph.D., Osama Mawlawi, Ph.D., Mark Slifstein, Ph.D., Justine Kent, M.D., Norman Simpson, B.S., Ramin V. Parsey, M.D., Ph.D., Tomoki Hashimoto, M.D., Yiyun Huang, Ph.D., Ann Shinn, B.S., Ronald Van Heertum, M.D., Anissa Abi-Dargham, M.D., Stephen Caltabiano, Ph.D., Andrea Malizia, M.D., Hugh Cowley, M.D., J. John Mann, M.D., and Marc Laruelle, M.D.

Augmentation of selective serotonin reuptake inhibitors (SSRIs) therapy by the 5-HT$_{1A}$ receptor agent pindolol may reduce the delay between initiation of antidepressant treatment and clinical response. This hypothesis is based on the ability of pindolol to block 5-HT$_{1A}$ autoreceptors in the dorsal raphe nuclei (DRN) and to potentiate the increase in 5-HT transmission induced by SSRIs. However, placebo-controlled clinical studies of pindolol augmentation of antidepressant therapy have reported inconsistent results. Here, we evaluated the occupancy of 5-HT$_{1A}$ receptors during treatment with pindolol controlled release (CR) in nine healthy volunteers with Positron Emission Tomography and [^{11}C]WAY 100635. Subjects were studied four times: at baseline, following one week of pindolol CR 7.5 mg/day (4 and 10 hrs post dose), and following one dose of pindolol CR 30 mg(4 hrs post dose). Occupancy of the DRN was 40 $\pm$ 29% on scan 2, 38 $\pm$ 26% on scan 3, and 64 $\pm$ 15% on scan 4. The average occupancy in all other regions was significantly lower at each doses (18 $\pm$ 5% on scan 2, 12 $\pm$ 3% on scan 3, and 42 $\pm$ 4% on scan 4). These results suggest that the blockade in the DRN reached in clinical studies (7.5 mg/day) might be too low and variable to consistently augment the therapeutic effect of SSRIs. However, these data indicate that pindolol exhibits in vivo selectivity for the DRN 5-HT$_{1A}$ autoreceptors. As DRN selectivity is desirable for potentiation of 5-HT function, this observation represents an important proof of concept for the development of 5-HT$_{1A}$ agents in this application.
[Neuropsychopharmacology 24:209–229, 2001]
© 2001 American College of Neuropsychopharmacology.
Published by Elsevier Science Inc.

The antidepressant effect of the selective serotonin reuptake inhibitors (SSRIs) is thought to be mediated by enhanced serotonin (5-HT) transmission. However, initial exposure to SSRIs is associated with no change or even a decrease in extracellular 5-HT levels in the terminal fields of the forebrain (Chaput et al. 1986; Invernizzi et al. 1992;

NEUROPSYCHOPHARMACOLOGY 2001–VOL. 24, NO. 3
© 2001 American College of Neuropsychopharmacology
Published by Elsevier Science Inc.
655 Avenue of the Americas, New York, NY 10010

0893-133X/01/$–see front matter
PII S0893-133X(00)00187-1

Romero et al. 1996; Gartside et al. 1999), due to stimulation by 5-HT of somatodendritic 5-HT_{1A} autoreceptors in the dorsal raphe nuclei (DRN), the major source of serotonin fibers to the forebrain (for review see Artigas et al. 1996). An acute increase of extracellular 5-HT in the DRN activates the 5-HT_{1A} autoreceptors and decreases the firing rate of the 5-HT neurons (Bel and Artigas 1992; Invernizzi et al. 1992). Electrophysiologic rodent studies suggest that with continued administration of SSRIs the 5-HT_{1A} autoreceptors become desensitized, resulting in enhanced 5-HT transmission after two to three weeks of treatment, a time frame which approximates the time of onset of the antidepressant effect (for reviews see Blier and de Montigny 1994; Artigas et al. 1996).

In rodents, blockade of the DRN 5-HT_{1A} autoreceptors prevents the immediate reduction in 5-HT transmission and potentiates the effects of SSRIs (Invernizzi et al. 1992; Dreshfield et al. 1996; Hjorth 1996; Romero et al. 1996; Maione et al. 1997; Gartside et al. 1999). This observation led to the hypothesis that blockade of the 5-HT_{1A} autoreceptors might decrease the latency to clinical improvement by antidepressant pharmacotherapy. Pindolol is a β-adrenergic receptor antagonist with affinity for the 5-HT_{1A} receptor (Hoyer and Schoeffter 1991). Initial open label clinical studies reported that the co-administration of pindolol with SSRI enhanced and/or accelerated the antidepressant effects of the SSRIs (Artigas et al. 1994; Blier and Bergeron 1995; Bakish et al. 1997). However, the results of subsequent double-blind controlled trials have been less consistent (Maes et al. 1996, 1999; Berman et al. 1997, 1999; Perez et al. 1997, 1999; Tome et al. 1997; Zanardi et al. 1997, 1998; Bordet et al. 1998).

The dose of pindolol used in clinical studies was generally 2.5 mg three times per day (t.i.d.), i.e., 7.5 mg per day. This dose was chosen due to the low incidence of cardiovascular side effects (doses of 30 to 45 mg/day are typically used for antihypertensive therapy) (Aellig et al. 1982). However, the degree of blockade at the 5-HT_{1A} receptors produced by this dose of pindolol (7.5 mg/day) is unknown, and the mixed clinical findings might result from a low or variable blockade of 5-HT_{1A} receptors.

In this study, the occupancy of 5-HT_{1A} receptors by various regimens of pindolol was assessed with positron emission tomography (PET) and the radiolabeled 5-HT_{1A} antagonist [*carbonyl*-^{11}C]WAY 100635 (denoted here [^{11}C]WAY 100635) in nine healthy volunteers. WAY-100635 [N-(2-(4-(2-methoxyphenyl)-1-piperazinyl)ethyl)-N-(2-pyridinyl) cyclohexane carboxamide] is a potent and selective 5-HT_{1A} antagonist with high affinity and selectivity for the 5-HT_{1A} receptors ($K_D = 0.1\text{-}0.4$ nM) (Forster et al. 1995; Gozlan et al. 1995). [^{11}C]WAY 100635 is a newly developed radiotracer that enables reliable quantification of 5-HT_{1A} receptor availability in the human brain (Pike et al. 1995; Farde et al. 1998; Gunn et al. 1998; Drevets et al. 1999; Parsey et al. 2000; Sargent et al. 2000).

Preclinical studies also indicate that pindolol might be more potent at blocking the DRN 5-HT_{1A} autoreceptors than the postsynaptic 5-HT_{1A} receptors in cortical and limbic areas (Romero et al. 1996; Tada et al. 1999). This property of pindolol might be of importance for augmenting the antidepressant effects of SSRIs, in that pindolol may block autoreceptor activation in the DRN without interfering with 5-HT transmission at the 5-HT_{1A} receptors in the terminal fields. Yet, not all preclinical results agree with a preferential effect of pindolol on somatodendritic 5-HT_{1A} autoreceptor (Corradetti et al. 1998). Therefore, the second aim of this study was to clarify this question by comparing the 5-HT_{1A} receptor occupancy of varying doses of pindolol in the DRN and in several neocortical regions in healthy human volunteers.

MATERIALS AND METHODS

General Design

The general design of the study is presented in Figure 1. Following screening and written informed consent, subjects first underwent a baseline [^{11}C]WAY 100635 PET scan (scan 1) and an MRI scan. Approximately five days later, subjects were started on pindolol controlled release (CR) for a total of nine days. Because of its short half-life (3 to 4 h) (Borchard 1990), pindolol is usually given t.i.d.. We employed a new formulation of the drug which allows once daily dosing (pindolol CR) that matches the drug exposure of t.i.d. dosing with the immediate release formulation. From Days 1 to 7, subjects received pindolol CR 7.5 mg p.o. q.d. at 8 A.M.. On Day 6, subjects were admitted to the Biological Studies Unit (BSU) at New York State Psychiatric Institute for four nights (Days 6–10). Two [^{11}C]WAY 100635 PET scans were performed on Day 7, at noon (scan 2, 4 h post dose) and 6 P.M. (scan 3, 10 h post dose). On Day 8, the dose of pindolol CR was increased to 22.5 mg p.o. q.d. at 8 A.M. On Day 9, the dose of pindolol CR was further increased to 30 mg p.o. q.d. at 8 A.M., and a PET scan was obtained at noon (scan 4, 4 h post dose). On Day 10, subjects were discharged from the hospital, and a follow-up visit took place on Day 14.

Subjects

To avoid potential effects of the menstrual cycle on 5-HT_{1A} receptors, only male subjects were recruited for this study. The absence of medical, neurological and psychiatric history (including alcohol and drug abuse) was assessed by history, review of systems, physical examination, routine blood tests, urine toxicology, EKG and spirometry. The study was approved by Columbia Presbyterian Medical Center and New York State Psychiatric Institute Institutional Review Boards.
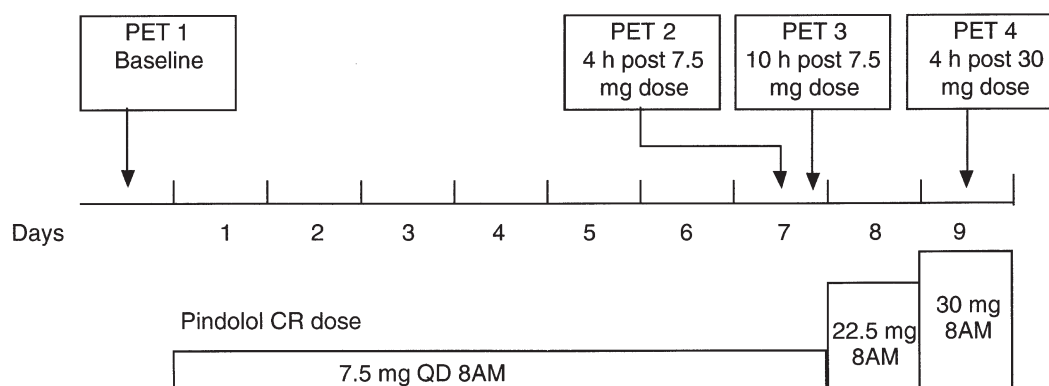
Figure 1. General design of the study. Following a baseline PET [^{11}C]WAY 100635 scan, subjects were started on pindolol controlled release (CR) 7.5mg p.o. q.d.. On Day 7, PET scans 2 and 3 were obtained at 4 h and 10 h post dose, respectively. On Days 8 and 9, the doses were increased to 22.5 mg p.o. q.d. and 30 mg p.o. q.d., respectively. PET scan 4 was obtained on Day 9 at 4 h post dose.

We report here the results of 33 scans in nine subjects. Eleven subjects (age of 35.2 ± 8.8 y.o.) participated in this study. Two subjects were excluded from the study after the baseline scan (one subject decided to withdraw, and the second was excluded due to an inability to tolerate the head restraining device used in the scanner). Therefore, nine subjects started and completed the pindolol treatment. Three scans were not obtained (scan 2 of subject 6, scan 3 of subject 9, and scan 4 of subject 7), due to low radiochemical yield (n = 2) or cyclotron down time (n = 1). Thus, a complete dataset (4 of 4 scans) was acquired in six subjects, and an incomplete data set (3 of 4 scans) was obtained in three subjects.

Radiochemistry

[^{11}C]WAY 100635 was prepared with a modification (Hwang et al. 1999) of the previously published method (Osman et al. 1996). Table 1 provides the mean, SD, and range of injected doses (ID) and specific activities at time of injection (SA) for each scan. No difference was observed in ID or SA between the 4 scan conditions (repeated measures ANOVA, p = .34 and p = .39, respectively), and no relationship was observed between [^{11}C]WAY 100635 injected masses and measured pindolol occupancies in scans 2, 3, and 4. Effective time of [^{11}C]WAY 100635 injections were 288 ± 39 min, 620 ±

42 min and 285 ± 87 min post pindolol dose for scans 2, 3, and 4, respectively.

PET Protocol

PET imaging sessions were conducted as previously described (Parsey et al. 2000). Subject preparation included placement of arterial and venous catheters, fiducial markers and polyurethane head immobilizer. An arterial catheter was inserted in the radial artery after completion of the Allen test and infiltration of the skin with 2% lidocaine. A venous catheter was inserted in a forearm vein on the opposite side. Four fiducial markers filled with C-11 (about 2 μCi /marker at time of injection) were glued on the subject's head. A polyurethane head immobilizer system (Soule Medical, Tampa, FL) was used to minimize head movement (Mawlawi et al. 1999). PET imaging was performed with the ECAT EXACT HR+ (Siemens/CTI, Knoxville, TN) (63 slices covering an axial field of view of 15.5 cm, axial sampling of 2.46 mm, in plane and axial resolution of 4.4 and 4.1 mm full width half-maximum at the center of the field of view in the 3 D mode, respectively). A 10-min transmission scan was obtained prior to radiotracer injection. [^{11}C]WAY 100635 was injected i.v. over a 45-sec period. Emission data were collected in the 3D mode for 100 min as 19 successive frames of increasing

Table 1. Injected Dose and Specific Activities of [^{11}C]WAY 100635

		Scan 1	Scan 2	Scan 3	Scan 4
Injected Dose (mCi)	Mean ± SD	13.1 ± 3.5	9.8 ± 3.6	13.8 ± 2.8	10.3 ± 4.0
	Range	5.7–17.7	4.5–15.5	7.7–17.1	4.3–15.6
Specific activity (Ci/mmoles)	Mean ± SD	2889 ± 1838	2349 ± 1074	3291 ± 867	3332 ± 1296
	Range SA	858–7103	1122–4107	1797–4674	1681–6070

ID expressed in mCi; SA expressed in Ci/mmoles.

duration (3 * 20 s, 3 * 1 min, 3 * 2 min, 2 * 5 min, 8 * 10 min). Images were reconstructed with attenuation correction using the transmission data and a Sheppe 0.5 filter (cutoff 0.5 cycles/projection rays).

Input Function Measurement

Following radiotracer injection, arterial samples were collected every 10 sec with an automated sampling system for the first two minutes, and manually thereafter at longer intervals. A total of 30 samples were obtained per experiment. Following centrifugation (10 min at 1800g), a 200 μl aliquot of plasma was collected and activity measured in a gamma counter (Wallac 1480 Wizard 3M Automatic Gamma Counter).

Six selected samples (collected at 2, 6, 12, 20, 40, and 60 min) were further processed by protein precipitation using acetonitrile followed by high pressure liquid chromatography (HPLC) to measure the fraction of plasma activity representing unmetabolized parent compound. The HPLC system includes the Phenomenex C18 analytical column (10 micron, 4.6 × 250 mm), which was eluted with a mixture of acetonitrile (50%) and aqueous 0.1 M ammonium formate (50%) at a flow rate of 2 ml per min. Five fractions collected over 12 min were counted. A [11C]WAY 100635 standard was processed with each experiment and parent eluted with fractions 4 and 5. The fraction parent was estimated by the decay corrected ratio of activity in fractions 4 and 5 to the activity of the total collection.

The six measured fractions of parent compound were fitted to the sum of one exponential plus a constant in order to interpolate values between and after these measurements (Parsey et al. 2000). The input function was calculated as the product of the total counts and interpolated fraction of parent compound at each time. The measured input function values ($C_a(t)$, μCi mL^{-1}) were fitted to a sum of three exponentials, and the fitted values were used as input to the kinetic analyses. The clearance of the parent compound (C_L, L/h) was calculated as the ratio of the injected dose to the area under the curve of the input function (Abi-Dargham et al. 1994). Determination of [11C]WAY 100635 free fraction in the plasma was performed in triplicate by ultracentrifugation (Gandelman et al. 1994).

MRI Acquisition and Segmentation Procedures

MRIs were acquired on a GE 1.5 T Signa Advantage system. Following a sagittal scout (1 min), performed to identify the AC-PC plane, a transaxial T1 weighted sequence with 1.5 mm slice thickness was acquired in a coronal plane orthogonal to the AC-PC plane over the whole brain with the following parameters: 3-dimensional SPGR (Spoiled Gradient Recalled Acquisition in the Steady State); TR 34 msec; TE 5 msec; flip angle of 45 degrees; slice thickness 1.5 mm and zero gap; 124 slices; FOV 22 × 16 cm; with 256 × 192 matrix, reformatted to 256 × 256, yielding a voxel size of 1.5 mm × 0.9 mm × 0.9 mm; and time of acquisition 11 min. MRI segmentation was performed within MEDx (Sensor Systems, Inc., Sterling, Virginia), with original subroutines implemented in MATLAB (The Math Works, Inc., Natick, Massachusetts). Steps for MRI segmentation included correction for field inhomogeneities, fitting of the voxel distribution to a combination of 3 Gaussians functions, voxel classification and post filtering (see details in Abi-Dargham et al. 2000).

Image Analysis

Image analysis was performed with MEDx (Sensor Systems, Inc.) as follows: 1) Frame realignment was performed by aligning the fiducial markers to the coordinates of their location in the first frame. 2) Following frame to frame registration, the 19 frames were summed and the summed PET image was coregistered and resampled to the MRI, using the Automated Image Registration program (Woods et al. 1992). The summed PET image was used because it contains counts from the initial, flow dependent activity distribution which enhances detection of the boundaries of regions with low receptor density, such as the cerebellum. The parameters of the spatial transformation matrix of the summed PET data set were then applied to each individual frame. Thus, each PET frame was resampled in the coronal plane to a voxel volume of 1.5*0.9*0.9 mm^3. 3) Regional boundaries were drawn on the MRI according to criteria (available on request) based on brain atlases (Talairach and Tournoux 1988; Duvernoy 1991) and on published reports (Kates et al. 1997; Killiany et al. 1997).

Eleven regions of interest (ROIs) and one region of reference (cerebellum) were included in the analysis: dorsolateral prefrontal cortex (DLPFC, size of 46,586 ± 7748 mm^3, mean ± SD of nine subjects, sum of right and left), medial prefrontal cortex (MPFC, 13,650 ± 3438 mm^3), orbito-frontal cortex (OFC, 14,077 ± 5747 mm^3), subgenual prefrontal cortex (SGPFC, 2065 ± 273 mm^3), anterior cingulate cortex (ACC, 8591 ± 1,869 mm^3), parietal cortex (PAR, 76,007 ± 10,582 mm^3), temporal cortex (TEM, 70,421 ± 7134 mm^3), insular cortex (INS, 9869 ± 1505 mm^3), occipital cortex (OCC, 50,335 ± 9371 mm^3), medial temporal region (MTL, 22,265 ± 1846 mm^3), dorsal raphe nuclei (DRN, 2215 ± 755 mm^3) and cerebellum (CER, 73,087 ± 25,181 mm^3).

The MTL consisted of a spatially weighted average of five limbic structures (uncus, amygdala, entorhinal cortex, parahippocampal gyrus, and hippocampus). Caudate, putamen , and thalamus were analyzed but not reported, given the very low density of $5HT_{1A}$ receptors in these regions. The cerebellum was used as the region of reference, since this region is devoid of de-

tectable 5-HT$_{1A}$ receptors (Hoyer et al. 1986; Dillon et al. 1991; Farde et al. 1997; Hall et al. 1997). Right and left regions for bilateral ROIs were averaged.

The same ROI boundaries were used to analyze the four scans of a given subject. For cortical regions, "large" regions were first drawn on the MRI to delineate the boundaries of the ROIs. Within these regions, activity was measured only in the voxels classified as gray matter by the segmentation procedure (see details in Abi-Dargham et al. 2000). The advantage of the segmentation procedure is that it is operator-independent and much faster and reliable than manual tracing of gray/white/CSF boundaries. The subcortical regions were directly identified on the MRI and were not segmented. The DRN region was the only region not drawn on the MRI, due to the lack of identifiable boundaries that can be visualized on the MRI. The DRN region was drawn directly on PET scans in reference to the DRN activity concentration, and the same DRN region was used to analyse each of the scans.

Derivation of Regional Total Distribution Volumes

Derivation of [^{11}C]WAY 100635 regional distribution volumes was performed using kinetic analysis and a three compartment model (Mintun et al. 1984; Laruelle et al. 1994c; Parsey et al. 2000). The three compartment configuration included the arterial plasma compartment (C_a), the intracerebral free and nonspecifically bound compartment (nondisplaceable compartment, C_2), and the specifically bound compartment (C_3). Brain activity was corrected for the contribution of plasma activity assuming a 5% blood volume (Mintun et al. 1984).

The total regional distribution volume (V_T, mL of plasma/g of tissue) was defined as the ratio of the tracer concentration in this region to the metabolite-corrected plasma concentration at equilibrium

$$V_T = \frac{C_T}{C_a} \quad (1)$$

V_T is equal to the sum of the distribution volumes of the second (nondisplaceable, V_2) and third (specific, BP) distribution volumes. V_T was derived from the kinetic rate constants as

$$V_T = \frac{K_1}{k_2}\left(1 + \frac{k_3}{k_4}\right) \quad (2)$$

where K_1 (mL g^{-1} min^{-1}) and k_2 (min^{-1}) are the unidirectional fractional rate constants for the transfer between C_a and C_2, and k_3 (min^{-1}) and k_4 (min^{-1}) are the unidirectional fractional rate constants for the transfer between C_2 and C_3.

Kinetic parameters were derived by nonlinear regression using a Levenberg-Marquart least squares minimization procedure (Levenberg 1944) implemented in MATLAB (The Math Works, Inc., South Natick, MA) as

previously described (Laruelle et al. 1994b). Given the unequal sampling over time (increasing frame acquisition time from beginning to end of the study), the least squares minimization procedure was weighed by the square root of the frame acquisition time. The identifiability of the parameters was assessed by the standard error of the parameters at convergence, given by the diagonal of the covariance matrix (Carson 1986), and expressed as percent of the parameters (coefficient of variation, %CV).

Derivation of Binding Potential

The binding potential (BP) was derived as the difference between total (V_T) and nonspecific (V_2) distribution volumes, with cerebellum V_T used as a measure of V_2:

$$BP = V_T - V_2 \quad (3)$$

Under these conditions, BP is equal to (Laruelle et al. 1994c) :

$$BP = \frac{f_1 Bmax}{K_D} \quad (4)$$

where Bmax is the regional concentration of 5HT$_{1A}$ receptors (nM per g of tissue), K_D is the affinity of [^{11}C]WAY 100635 for 5HT$_{1A}$ receptors (nM per mL of brain water), and f_1 is the free fraction of [^{11}C]WAY 100635 in the plasma. While f_1 was measured in this study, the derivation of BP was not corrected for f_1, given the low free fraction of [^{11}C]WAY 100635 in the plasma ($< 10\%$) and the lack of reliability of f_1 measurement when f_1 is $< 10\%$ (Abi-Dargham et al. 2000; Parsey et al. 2000).

The use of the cerebellum [^{11}C]WAY 100635 V_T as an estimate of the nonspecific distribution volume is supported by the lack of detectable 5-HT$_{1A}$ receptors in the cerebellum (Dillon et al. 1991; Hoyer and Schoeffter 1991; Farde et al. 1997; Hall et al. 1997). Despite the absence of displaceable binding, kinetic modeling of the cerebellar uptake requires a two tissue compartment model (Farde et al. 1998; Gunn et al. 1998; Parsey et al. 2000). This second cerebellar tissue compartment likely reflects a kinetically distinguishable nonspecific binding or a slow buildup of radiolabeled metabolites in the brain (see full discussion in Parsey et al. 2000).

Another outcome measure of interest was the BP normalized to cerebellum, termed V_3'' or k_3/k_4 ratio. V_3'' is equal to the ratio of BP to V_2 (Laruelle et al. 1994c).

$$V_3'' = \frac{k_3}{k_4} = \frac{BP}{V_2} = \frac{Bmax}{V_2 K_D} = \frac{f_2 Bmax}{K_D} \quad (5)$$

where f_2 is the free fraction in the brain ($f_2 = 1/V_2$). Given the low value of V_2 for [^{11}C]WAY 100635 (less than unity), the reproducibility of V_3'' was found to be lower than the reproducibility of BP for [^{11}C]WAY 100635 (Parsey et al. 2000). Therefore, BP as defined by equation 4 was selected a priori as the outcome measure for this study.

Derivation of Occupancy

The occupancy achieved by pindolol during scan i (where i = 2, 3, or 4) was calculated as:

$$\text{Occupancy} = 100 \cdot \frac{BP_1 - BP_i}{BP_1} \qquad (6)$$

where BP_1 is BP measured during baseline scan (scan 1).

Pindolol Plasma Measurement

Blood sampling for determination of plasma pindolol levels was obtained on Days 7 and 9 at the following times: Day 7: Pre-dose, then 1, 2, 3, 4*, 5*, 6*, 8, 10*, 12*, 13, 14, 16, and 24 hours post-dose; Day 9: Pre-dose, then 1, 2, 3, 4*, 5*, 6*, 8, 10, 12, 16 and 24 hours post-dose, where * are the samples taken in association with the [¹¹C]WAY 100635 scans. Blood samples were centrifuged within 30 minutes after collection (1500g, 4°C), and plasma samples were frozen at −20°C until assays were performed at the Drug Analysis Department, SmithKline Beecham (Welwyn, UK).

Pindolol steady state pharmacokinetic parameters were calculated from the plasma concentrations, including the maximal and minimal concentration (C_{max} and C_{min}), the peak time (T_{max}), the area under the curve for 24 h [AUC(0–24)] and the average plasma concentrations (C_{av}) during the PET scans [AUC(4–6)/2 and AUC(10–12)/2] and during the dosing interval [AUC(0–24)/24]. Pindolol pharmacodynamic parameters (maximal effect, E_{max}, and pindolol concentration at half-maximal effect, EC_{50}) were obtained by fitting the function Occ = $E_{max}P/(EC_{50} + P)$ to data from scans 2 and 4, where P is pindolol plasma concentration (ng mL^{-1}) and Occ is receptor occupancy (%).

Statistical Analysis

Statistical analysis was performed with factorial or repeated measures ANOVA, as appropriate. Because of three missing values (one value missing on scans 2, 3, and 4, respectively), repeated measures ANOVA were performed only on the six subjects with complete data sets. This analysis was followed by pairwise comparisons, which included the whole data set ($n = 8$ per scans). All values are given as mean ± SD in the text and mean ± SEM in figures. Significance level was set at $p < .05$ and all contrasts were two tailed.

RESULTS

[¹¹C]WAY 100635 Plasma Analysis

[¹¹C]WAY 100635 clearance rate from plasma was unaffected by pindolol treatment (scan 1: 181 ± 19 L/h; scan 2: 177 ± 16 L/h; scan 3: 176 ± 24 L/h; scan 4: 181 ± 23 L/h; repeated measures ANOVA, $p = .68$). The presence of pindolol significantly increased [¹¹C]WAY 100635 plasma free fraction (scan 1: 3.5 ± 0.6%; scan 2: 4.4 ± 0.8%; scan 3: 4.6 ± 1.7%; scan 4: 4.6 ± 1.4%, repeated measures ANOVA, $n = 6$, $p = .012$). Post-hoc analysis revealed that the increase in f_1 reached significance on scans 2 and 4, the two conditions expected to have the highest pindolol plasma concentration (scan 1 versus scan 2, $n = 8$, $p = .049$; scan 1 versus scan 3, $n = 8$, $p = .13$; scan 1 versus scan 4, $n = 8$, $p = .023$).

Brain Analysis

In general, the regional V_T values were well identified by the three compartment analysis. The average error on the estimation of V_T was 6.8 ± 11.2% ($n = 396$, 12 regions * 33 scans). Significant between region differences were observed in the identifiability of V_T (repeated measures ANOVA with regions as repeated measures, $p = .009$). Post-hoc analysis revealed that DRN V_T had a higher uncertainty (identifiability of 32 ± 27%) compared to other regions (4.6 ± 3.5%, $p < .001$).

No effect of pindolol was observed on the cerebellum V_T (Table 2), an observation consistent with the lack of 5HT$_{1A}$ receptors in this region (repeated measures ANOVA, $p = 0.21$) and supporting the use of this region to measure nonspecific distribution volume. This was confirmed on pairwise comparisons (scans 1 versus 2, 3, and 4: $p = .80$, .43, and .29, respectively).

Regional BP was calculated as the difference between the regional V_T and cerebellar V_T (Table 3). A significant decrease in regional BP was observed with pindolol administration (repeated measures ANOVA, $n = 66$, $p < .001$) (Figure 2). This decrease was observed for each scan (repeated measures ANOVA, $n = 88$, $p < .001$ for all three contrasts). BP values during scan 2 were lower than during scan 3 ($n = 88$, $p < .001$), which was consistent with the observation that pindolol blood levels were higher at 4 h compared to 10 h after administration.

Table 4 lists the occupancy by region (average of all subjects) measured during scans 2, 3, and 4. Combining

Table 2. Cerebellum [¹¹C]WAY 100635 V_T (ml g^{-1}) During the Four Conditions

Subject #	Scan 1	Scan 2	Scan 3	Scan 4
1	0.60	0.45	0.45	0.29
2	0.62	0.63	0.50	0.61
3	0.97	1.06	1.01	0.57
4	0.70	0.50	0.51	0.56
5	0.49	0.49	0.63	0.53
6	0.34	–	0.30	0.28
7	0.30	0.33	0.33	–
8	0.31	0.33	0.34	0.31
9	0.22	0.35	–	0.47
Mean ± SD	0.51 ± 0.24	0.52 ± 0.24	0.51 ± 0.23	0.45 ± 0.14

Table 3. Regional [^{11}C]WAY 100635 BP (ml g^{-1}) During Four Scan Conditions

Subject #	Scan #	DLPFC	MPFC	OFC	SGPFC	ACC	TEM	INS	PAR	OCC	MTL	DRN
1	1	2.42	2.46	1.77	2.01	2.68	4.11	4.64	2.38	2.13	7.34	1.82
	2	2.36	2.49	1.92	2.41	2.63	3.66	4.03	2.11	1.86	5.20	1.65
	3	2.65	2.79	1.79	1.74	2.76	3.89	4.48	2.42	1.98	5.07	1.28
	4	1.41	1.63	1.94	1.42	1.45	2.62	2.63	1.20	0.88	4.04	0.42
2	1	3.43	4.06	3.39	4.56	4.41	5.40	6.12	2.99	2.74	5.97	2.45
	2	1.62	2.18	1.84	2.73	2.29	3.04	3.02	1.42	1.39	3.03	0.80
	3	2.57	3.04	2.83	3.36	3.30	3.94	4.46	2.20	1.95	3.80	1.62
	4	1.37	1.81	1.35	1.75	1.77	2.28	2.24	1.18	1.05	2.40	0.80
3	1	1.60	1.88	1.58	1.39	1.68	3.06	3.08	1.77	1.27	3.78	3.85
	2	1.78	2.09	2.22	2.03	1.79	3.41	3.62	1.75	1.31	3.90	0.90
	3	1.69	1.94	1.93	1.48	1.59	3.14	3.99	1.80	1.24	3.68	1.19
	4	0.96	1.15	1.11	1.18	1.03	1.94	2.09	1.01	0.82	2.23	0.65
4	1	4.67	5.27	4.84	5.19	5.49	6.72	8.04	3.77	3.06	8.35	2.31
	2	2.70	3.28	2.56	4.57	3.32	3.84	4.92	2.19	1.71	4.74	1.31
	3	3.04	3.68	3.25	5.12	3.95	4.86	6.33	2.39	2.33	5.46	1.60
	4	2.72	3.09	2.72	3.76	2.98	3.87	4.32	2.03	1.75	3.60	1.48
5	1	3.11	3.30	3.21	3.98	3.94	5.00	5.56	2.27	2.06	4.16	2.53
	2	2.34	2.83	2.70	2.82	2.97	4.08	4.56	2.02	1.66	5.28	0.74
	3	3.09	3.48	3.07	4.21	3.63	4.45	5.58	2.39	2.09	6.10	1.44
	4	1.64	1.86	1.75	2.30	2.06	2.85	3.08	1.29	1.08	3.82	0.64
6	1	1.89	2.50	1.36	2.82	2.61	2.85	3.22	1.38	1.40	2.59	2.92
	2	—	—	—	—	—	—	—	—	—	—	—
	3	1.59	1.88	1.57	2.23	1.71	2.00	2.06	1.36	0.92	2.38	0.63
	4	1.14	1.25	1.10	1.58	1.36	1.78	1.85	0.92	0.81	1.92	1.04
7	1	2.41	2.81	2.68	3.46	2.83	3.65	4.25	2.11	1.62	4.85	1.38
	2	2.03	2.44	2.18	2.85	2.31	2.97	3.45	1.73	1.16	3.91	1.23
	3	1.75	2.08	1.77	2.56	2.19	2.82	3.07	1.50	1.00	3.70	1.03
	4	—	—	—	—	—	—	—	—	—	—	—
8	1	2.37	2.74	2.36	3.11	2.97	3.41	3.88	1.96	1.68	4.42	1.51
	2	1.96	2.37	2.28	2.46	2.43	3.11	2.90	1.48	1.21	3.12	1.37
	3	2.16	2.61	2.09	3.37	2.99	3.24	3.77	1.80	1.86	3.94	1.60
	4	1.31	1.63	1.41	1.77	1.74	2.02	2.22	1.23	0.93	2.62	0.72
9	1	1.54	1.71	1.74	2.04	1.68	2.40	2.30	1.36	1.17	2.88	1.60
	2	1.22	1.39	1.47	1.97	1.46	2.19	2.03	1.12	1.11	2.59	1.13
	3	—	—	—	—	—	—	—	—	—	—	—
	4	0.82	0.90	0.99	1.51	1.07	1.67	1.43	0.69	0.83	1.97	0.68

DLPFC, dorsolateral prefrontal cortex; MPFC, medial prefrontal cortex; OFC, orbito-frontal cortex; SGPFC, subgenual prefrontal cortex; ACC, anterior cingulate cortex; TEM, temporal cortex; INS, insular cortex; PAR, parietal cortex; OCC, occipital cortex; MTL, medial temporal lobe; DRN, dorsal raphe nuclei.

all regions, occupancy was 20 ± 8% at scan 2, 14 ± 8% at scan 3 and 44 ± 8% at scan 4. Significant between region differences in occupancy were noted (repeated measures ANOVA: all scans, $n = 6$ subjects, $p < .0001$). This significant between region difference was present at each dose, and significant between region differences in occupancy was observed whether we included or excluded subjects with missing data point (results including all subjects: scan 2: $n = 8$, $p = .012$; scan 3: $n = 8$, $p = .011$; scan 4: $n = 8$, $p < .0001$). Pair-wise analyses revealed that occupancy in the DRN was higher than occupancy in all other regions for each scan ($p < .05$ for scans 2, 3, and 4, $n = 8$ per doses), but that other regions (corticolimbic regions) did not differ from each other (Figure 3). Thus, DRN occupancy was 40 ± 29% on scan 2, 38 ± 26% on scan 3, and 64 ± 15% on scan 4. The average occupancy in all other regions was 18 ± 5% on

scan 2, 12 ± 3% on scan 3, and 42 ± 4% on scan 4. Therefore, DRN occupancy was greater than the occupancy in the other regions by a factor of 2.2 on scan 2, 3.1 on scan 3, and 1.5 on scan 4.

Table 5 lists the average occupancy by subject (DRN occupancy and average of all other regions) measured during scans 2, 3, and 4. Large between subjects differences were observed in pindolol occupancy. This between subject variability was more pronounced following the low dose pindolol (scan 2 and 3) compared to the high dose (scan 4). This dose-dependent decrease in between subject binding variability is consistent with a saturation curve (at low dose, very small differences in ligand concentration will result in large differences in binding; at higher doses, large differences in ligand concentration will result in small differences in binding). A significant interaction was observed between
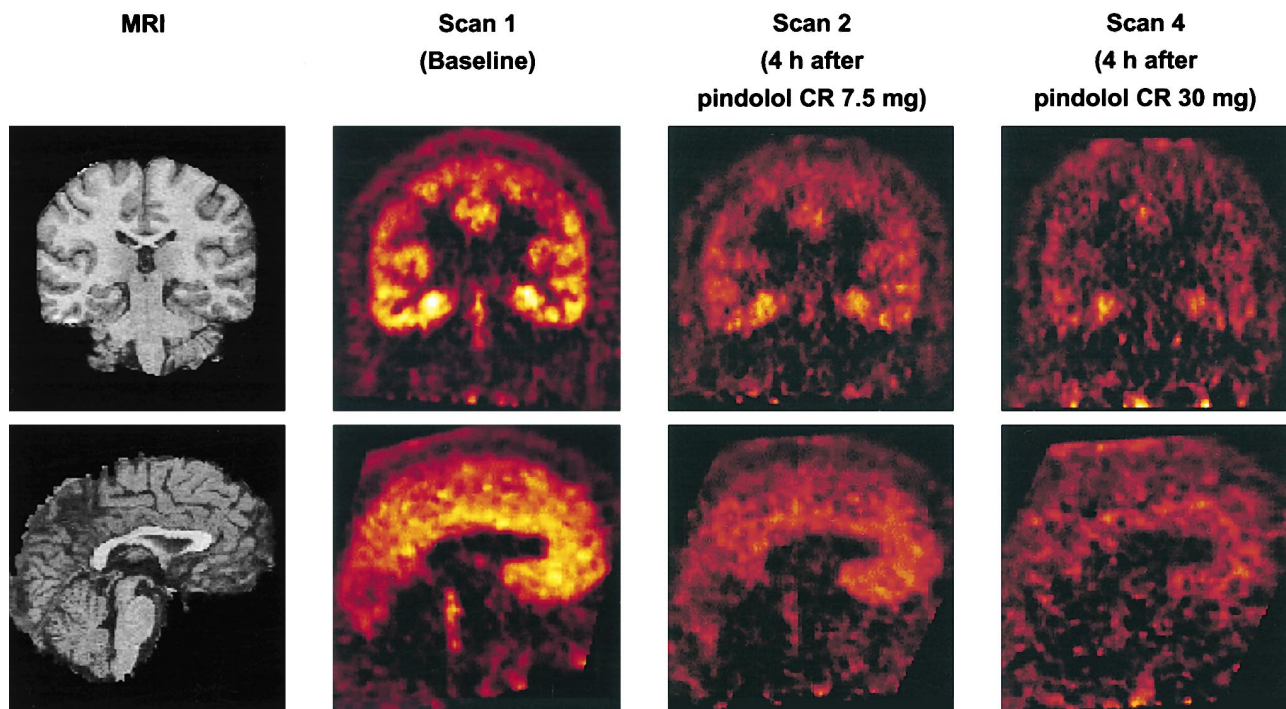
Figure 2. Coronal (top row) and sagittal (bottom row) MRI and coregistered PET images following injection of [^{11}C]WAY 100635 in subject 2 during scans 1, 2, and 4. The PET image is the sum of five frames of 10 min collected between 30 min and 80 min. Activity was corrected for the injected dose and color coded using the same scale across the three scans.

subjects and occupancy (repeated measures ANOVA with regional occupancy as repeated measures and subject as cofactor; subject * occupancy interaction: $p < .001$). Regional occupancies measured on scan 2 were predictive of the occupancies measured on scan 3 ($n = 77$, $r^2 = 0.57$, $p < .001$) and 4 ($n = 77$, $r^2 = 0.51$, $p < .001$).

Because of the significant differences in f_1 due to pindolol, occupancy was also computed using BP corrected for f_1 (derived as BP/f_1). Using this outcome measure, average regional occupancies were $34 \pm 6\%$ at scan 2, $25 \pm 8\%$ at scan 3, and $55 \pm 6\%$ at scan 4 (Table 6). These occupancies were higher than occupancies cal-

culated using BP as outcome measure, and the differences in estimated occupancy derived with these two outcome measures reached significance on scan 4 (paired t-test, $p = .04$), but not on scan 2 ($p = .07$), or scan 3 ($p = .22$). However, the f_1-corrected cerebellar V_T was significantly affected by scan conditions: cerebellum V_T/f_1 was 14.4 ± 7.5 ml g^{-1} on scan 1, 12.1 ± 6.6 ml g^{-1} on scan 2, 11.9 ± 6.1 ml g^{-1} on scan 3, and 10.0 ± 2.2 ml g^{-1} on scan 4 (repeated measures ANOVA, $p = .009$). This apparent decrease in cerebellum V_T/f_1 by pindolol was inconsistent with the lack of detectable 5-HT$_{1A}$ receptors in this region (Hoyer et al. 1986; Dillon

Table 4. Occupancy of 5HT$_{1A}$ Receptors by Pindolol: Regional Differences

Region	Scan 2	Scan 3	Scan 4
Dorsolateral prefrontal cortex	$20 \pm 20\%$	$12 \pm 16\%$	$45 \pm 7\%$
Medial prefrontal cortex	$16 \pm 19\%$	$11 \pm 17\%$	$44 \pm 7\%$
Orbitofrontal cortex	$12 \pm 29\%$	$8 \pm 20\%$	$34 \pm 21\%$
Subgenual prefrontal cortex	$7 \pm 28\%$	$8 \pm 15\%$	$36 \pm 15\%$
Anterior cingulate cortex	$20 \pm 18\%$	$15 \pm 14\%$	$45 \pm 7\%$
Temporal cortex	$18 \pm 18\%$	$16 \pm 13\%$	$41 \pm 8\%$
Insula	$20 \pm 20\%$	$11 \pm 21\%$	$44 \pm 9\%$
Parietal cortex	$22 \pm 17\%$	$12 \pm 16\%$	$45 \pm 8\%$
Occipital cortex	$23 \pm 18\%$	$15 \pm 18\%$	$45 \pm 11\%$
Medial temporal cortex	$19 \pm 25\%$	$13 \pm 27\%$	$39 \pm 17\%$
Dorsal raphe nuclei	$40 \pm 29\%$*	$38 \pm 26\%$*	$64 \pm 15\%$*
All regions (mean $\pm$ SD)	$20 \pm 8\%$	$14 \pm 8\%$	$44 \pm 8\%$

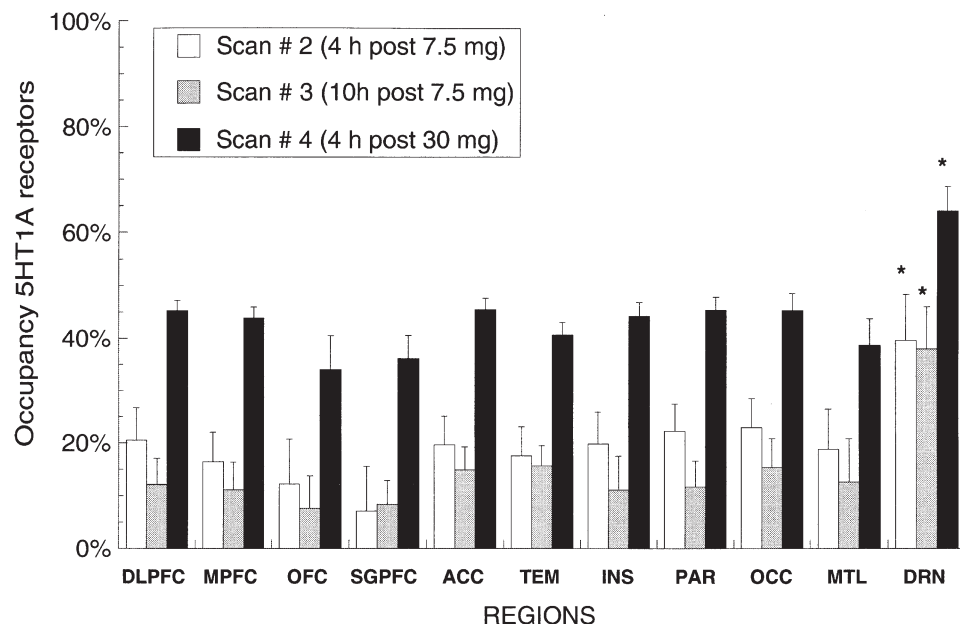*$p < .01$ compared to all other regions.

Figure 3. Occupancy of 5HT$_{1A}$ receptors by pindolol during scans 2, 3, and 4 in eleven regions of the human brain: dorsolateral prefrontal cortex (DLPFC), medial prefrontal cortex (MPFC), orbito-frontal cortex (OFC), subgenual prefrontal cortex (SGPFC), anterior cingulate cortex (ACC), parietal cortex (PC), temporal cortex (TC), insula (INS), occipital cortex (OC), medial temporal region (MTL), and dorsal raphe nuclei (DRN). Values are mean ± SEM. Occupancy was significantly higher in the DRN compared to other regions (* = $p < .05$).

et al. 1991; Farde et al. 1997; Hall et al. 1997), and raised doubt about the appropriateness of the f_1 correction. Therefore, occupancy in the other regions might be overestimated when BP is corrected for f_1.

Occupancy values derived with V_3'' are also provided in Table 6, and indicates a range of occupancy measurements similar to those obtained with BP. Occupancies derived with BP or V_3'' were not significantly different (paired t-tests, scan 2: $p = .16$; scan 3: $p = .15$; scan 4: $p = .08$).

Pindolol Plasma Measurement

Figure 4 shows the average pindolol plasma concentration during the 24 h following administration of pindolol 7.5 mg on Day 7 (scans 2 and 3) and 30 mg (scans 4) on Day 9. The pharmacokinetic parameters for Days 7 and 9 are presented in Table 7 and Table 8, respectively. Average plasma pindolol concentration were 18 ±

8 ng mL^{-1}, 7 ± 3 ng mL^{-1} and 58 ± 24 ng mL^{-1} during scans 2, 3, and 4, respectively.

The relationship between pindolol plasma levels and 5-HT$_{1A}$ receptor occupancy was studied on data from scans 2 and 4 (both scans obtained 4 h after dose) (Figure 5). Because of significant differences in pindolol occupancy between the DRN and all other regions, DRN and corticolimbic curves were fit separately. E$_{max}$ values (± standard error) were 95 ± 23% and 53 ± 17% in DRN and postsynaptic regions, respectively. This result suggested that the sites occupied by pindolol in this range of plasma concentrations corresponded to the whole population of 5-HT$_{1A}$ receptors in the DRN (E$_{max}$ corresponded to 95 ± 23% of 5-HT$_{1A}$ receptors labeled by [^{11}C]WAY 100635), but only to about half of the receptors in the postsynaptic areas (E$_{max}$ = 53 ± 17% of 5-HT$_{1A}$ receptors labeled by [^{11}C]WAY 100635). In other words, these data suggested that all DRN 5-HT$_{1A}$ receptors, but only 50% of corticolimbic 5-HT$_{1A}$ receptors,

Table 5. Occupancy of 5HT$_{1A}$ Receptors by Pindolol: Between Subject Differences

Condition Region	Scan 2		Scan 3		Scan 4	
	DRN	Other regions	DRN	Other regions	DRN	Other regions
Subject 1	9%	5 ± 14%	30%	3 ± 13%	77%	37 ± 19%
Subject 2	67%	48 ± 4%	34%	26 ± 5%	67%	60 ± 2%
Subject 3	77%	−15 ± 16%	69%	−6 ± 11%	83%	35 ± 8%
Subject 4	43%	39 ± 10%	31%	27 ± 10%	36%	43 ± 7%
Subject 5	71%	15 ± 16%	43%	−4 ± 16%	75%	41 ± 12%
Subject 6	—	—	78%	19 ± 17%	64%	38 ± 10%
Subject 7	11%	19 ± 4%	26%	28 ± 5%	—	—
Subject 8	9%	19 ± 8%	−6%	3 ± 8%	52%	42 ± 2%
Subject 9	29%	12 ± 6%	—	—	58%	38 ± 8%
Average ± SD (%CV)	40 ± 29% (73%)	18 ± 19% (109%)	38 ± 26% (69%)	12 ± 15% (121%)	64 ± 15% (24%)	42 ± 8% (19%)

Table 6. Occupancy of 5HT$_{1A}$ Receptors by Pindolol and Outcome Measures (All Regions)

Outcome measure	Scan 2	Scan 3	Scan 4
BP	20 ± 8%	14 ± 8%	44 ± 8%
BP/f$_1$	34 ± 6%	25 ± 8%	55 ± 6%
V$_3$"	19 ± 8%	9 ± 9%	31 ± 11%

were configured in a state of high affinity for pindolol. EC$_{50}$ values were 24 ± 15 ng mL^{-1} for the DRN and 21 ± 18 ng mL^{-1} in postsynaptic regions. Thus, no difference was observed in the pindolol concentration needed to occupy 50% of the high affinity sites in the DRN and postsynaptic regions (equivalent to the K$_D$ relative to total plasma concentration).

We also performed a fit with E$_{max}$ constrained to 100% (Table 9). In the DRN, the constrained fit (r = 0.68) was equivalent to the unconstrained fit (r = 0.68), and returned similar parameters (EC$_{50}$ = 27 ± 6 mg mL^{-1}). In corticolimbic regions, the constrained fit (r = 0.38) had a lower goodness of fit compared to the unconstrained fit (r = 0.50), and returned an EC$_{50}$ of 80 ± 16 ng mL^{-1}. The absence of data at higher receptor occupancy in the postsynaptic regions precluded formal comparison of both models.

DISCUSSION

The results of this study demonstrate a significant occupancy of the 5-HT$_{1A}$ receptor by pindolol in the human brain in vivo, and that this occupancy varies as expected with respect to dosage and blood levels. Across all brain regions the occupancy of pindolol was 20 ± 8% at the peak plasma level of the 7.5 mg dose, 14 ± 8% at 10 hrs following the 7.5 mg dose, and 44 ± 8% at the

peak of the 30 mg dose. Interestingly, the 5-HT$_{1A}$ receptor occupancy by pindolol was significantly higher in the DRN than in terminal fields of the neocortex and limbic regions. The DRN selectivity of pindolol suggested by this study supports its use as a pharmacological augmentation strategy in the treatment of depression. However, before accepting this conclusion, we must carefully consider potential sources of artifact in our results. These potential sources are noise in the DRN BP determination, partial voluming, ROI definition, regional variability in nonspecific binding and the potential effect of endogenous 5-HT on [^{11}C]WAY 100635 binding.

Potential Sources of Artifactual Results

Noise and Bias.   The first potential source of artifact we must consider is the difficulty in measuring DRN [^{11}C]WAY 100635 BP with PET. Measurement noise was assessed by the residual sum of squares (RSS) of the kinetic analysis, and was the highest in the DRN (DRN RSS = 0.0095 ± 0086 μCi^2/ml^2, n = 33; all other ROIs RSS = 0.0028 ± 0.0024 μCi^2/ml^2, n = 330). The identifiability of DRN BP was lower (error of 32 ± 27%) compared to the other ROIs (5 ± 3%). We previously reported that the test/retest variability of [^{11}C]WAY 100635 BP (calculated as the absolute difference between BP$_{test}$ and BP$_{retest}$ divided by their average) was ± 21 ± 22% in the DRN (5 pairs) compared to ± 9 ± 3% in cortical regions (Parsey et al. 2000).

The intraclass correlation coefficient (ICC) of BP was only 0.44 in the DRN, compared to 0.95 ± 0.01 in cortical regions. Similar values were reported by Gunn et al. (1998). Yet, the noise associated with measurement of the DRN BP is not expected, per se, to bias the results. It increases the likelihood of both type I and type II errors. Significantly higher occupancy in the DRN was ob-
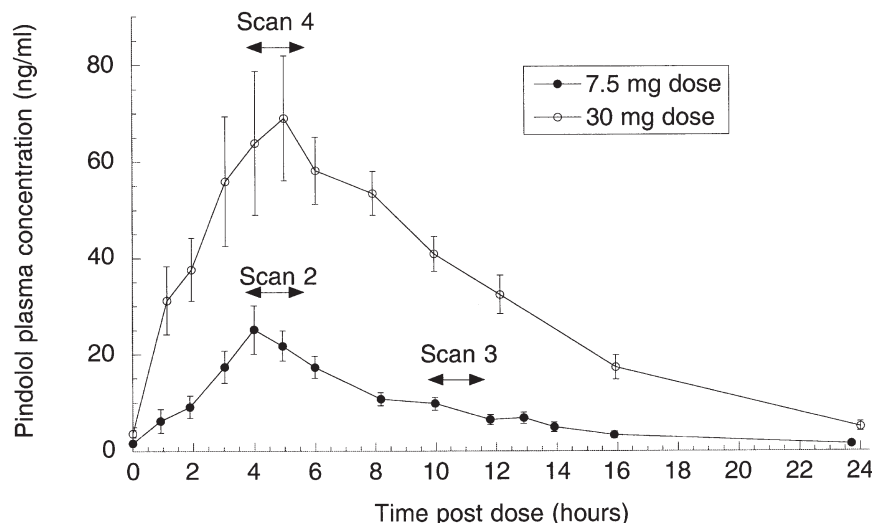

Figure 4. Pindolol plasma concentrations over time following doses of 7.5. mg CR p.o. (closed circles) and 30 mg CR p.o. (open circles). Values are mean ± SEM of nine subjects (value of 0.5 ng mL^{-1} were used when pindolol levels were below detection limits). The figure also depicts the timing of scans 2 and 3 relative to time post 7.5 mg dose, and scan 4 relative to time post 30 mg dose.

Table 7. Pindolol Plasma Measurements (Day 7, 7.5 mg Dose)

Subject	C$_{max}$ (ng mL^{-1})	T$_{max}$ (h)	AUC (0–24) (ng h mL^{-1})	C$_{min}$ (ng mL^{-1})	C$_{av}$** (Scan 2) (ng mL^{-1})	C$_{av}$** (Scan 3) (ng mL^{-1})	C$_{av}$** (0–24 h) (ng mL^{-1})
Subject 1	20.14	4.42	260.73	1.88	17.11	10.05	10.86
Subject 2	23.17	4.88	223.08	2.56	20.12	9.50	9.30
Subject 3	42.44	3.67	286.94	2.19	29.93	8.26	11.96
Subject 4	23.32	3.75	137.22	<LLQ	12.28	5.96	5.72
Subject 5	42.81	4.71	175.62	<LLQ	18.85	6.39	7.32
Subject 6	43.58	3.88	280.67	2.59	—	10.34	11.69
Subject 7	29.52	5.00	161.13	<LLQ	26.33	7.50	6.71
Subject 8	11.21	3.25	79.06	<LLQ	6.03	1.61	3.29
Subject 9	14.60	3.83	156.80	1.33	11.32	—	6.53
Average ± SD	28 ± 12	4 ± 1	196 ± 71	2 ± 1	18 ± 8	7 ± 3	8 ± 3

C$_{max}$, maximal concentration; T$_{max}$, time of maximal concentration; C$_{min}$, minimal concentration; LLQ = lower limit of quantification (1.00 ng mL^{-1}); AUC, area under the curve.

**C$_{av}$ = average pindolol plasma concentration (ng mL^{-1}) during a PET scan or a 24-hour dosing interval

served for each condition, making a chance finding (type I error) due to random noise in the measurement unlikely. This view is only valid if the noise does not produce a systematic bias in the outcome measure, and we have previously demonstrated that this condition is met for the analytical method used in this study, i.e. kinetic derivation of V$_T$ (Abi-Dargham et al. 2000).

Partial Voluming. The underestimation of BP by partial voluming is greater in the DRN than in the comparatively larger corticolimbic regions. Yet, the magnitude of the partial voluming effect is dependent on the volume of the structure and on the camera resolution, but not on the amount of activity (Kessler et al. 1984). Since the distance between DRN and other regions with specific binding exceeds two full width at half maximum (FWHM, ~ 5 mm), the DRN activity can be modeled as a small sphere surrounded by background nonspecific activity. Under these conditions, the relative underestimation of DRN BP due to partial voluming is the same at scans 1, 2, 3, and 4 and that partial voluming and

spill over does not bias measurement of occupancy (see appendix for theoretical demonstration).

This absence of bias was further demonstrated by computer simulations with a simulated image of 256 × 256 square pixels (pixel size of 0.78 mm2) including six "hot" spheres of various dimensions (diameters of 19.9, 17.3, 14.7, 11.9, 9.2, and 6.7 mm, respectively). Activities in the spheres and in the background were assigned levels of 1.4 and 0.5, respectively. To simulate various levels of occupancy by a competitive ligand, activities in the spheres were incrementally reduced from 1.4 to 0.5 (increments of 0.1). At each level of occupancy the image was blurred by a point spread function with FWHM ranging linearly from 4.3 to 8.15 mm in the radial direction and 4.3 to 5.0 mm in the tangential direction (these parameters closely approximate the spatially variant system resolution of the HR+ camera). The average activities in the blurred spheres were measured at each level of occupancy and occupancy was then computed according to Equation 6. Although measured activity levels were underestimated as the size of the

Table 8. Pindolol Plasma Measurements (Day 9, 30 mg Dose)

Subject	Cmax (ng mL^{-1})	T$_{max}$ (h)	AUC (0–24) (ng h mL^{-1})	C$_{min}$ (ng mL^{-1})	C$_{av}$** (Scan 4) (ng mL^{-1})	C$_{av}$** (0–24 h) (ng mL^{-1})
Subject 1	70.26	6.00	841.38	6.91	61.68	35.06
Subject 2	121.93	4.00	778.24 *	5.94	79.59	48.64 *
Subject 3	145.18	4.17	914.29 *	6.03	90.10	57.14 *
Subject 4	34.39	2.00	459.57	2.28	29.05	19.15
Subject 5	81.26	4.72	636.35	3.15	69.54	26.51
Subject 6	102.61	5.25	1007.82	6.90	66.69	41.99
Subject 7	53.52	0.92	708.24	3.20	—	29.51
Subject 8	55.97	3.83	574.97	2.50	46.03	23.96
Subject 9	45.73	8.08	420.98	2.14	22.41	17.54
Average ± SD	79 ± 37	4 ± 2	705 ± 201	4 ± 2	58 ± 24	28 ± 9

C$_{max}$, maximal concentration; T$_{max}$, time of maximal concentration; C$_{min}$, minimal concentration; LLQ = lower limit of quantification (1.00 ng mL^{-1}); AUC: area under the curve.

*AUC (0–16) and C$_{av}$ (0–16 h)—no sample at 24 h.

**C$_{av}$ = average pindolol plasma concentration (ng mL^{-1}) during a PET scan or a 24-hour dosing interval.
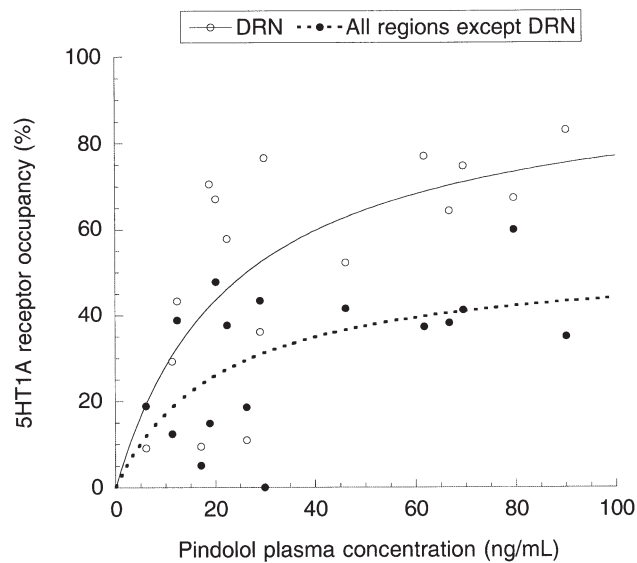
Figure 5. Relationship between pindolol plasma concentration at the time of the scan and occupancy of 5-HT$_{1A}$ in the DRN (open circles and solid line) and all postsynaptic regions (closed circles and dotted line). Pharmacodynamic parameters (E$_{max}$ and EC$_{50}$) were obtained by fitting the function Occ = E$_{max}$P/(EC$_{50}$ + P) to data from scans 2 and 4, where P is pindolol concentration (ng mL^{-1}) and Occ is receptor occupancy (%). Values (± standard error) of E$_{max}$ were 95 ± 23% and 53 ± 17% in DRN and postsynaptic regions, respectively. Values of EC$_{50}$ were 24 ± 15 ng mL^{-1} and 53 ± 21 ng mL^{-1}, in DRN and postsynaptic regions, respectively.

sphere decreased, measured occupancy agreed with the true occupancy to within 10^{-4} for all spheres at all levels of occupancy.

Next, a more realistic simulation was performed by simulating the activity concentrations over time in the background regions and in the spheres as if background and spheres activities represented a region of reference and region of interest, respectively. Background and spheres activities were created by the convolution of a typical [^{11}C]WAY 100635 input function and a one tissue compartment model for the background (K$_1$ = 0.069 mL g^{-1} min^{-1}; k$_2$ = 0.0902 min^{-1}) or a two tissue compartment for the spheres.

Two situations were simulated for the sphere activities, a "baseline scan" (K$_1$ = 0.069 mL g^{-1} min^{-1}; k$_2$ =

0.0902 min^{-1}; k$_3$ = 0.044 min^{-1}; k$_4$ = 0.014 min^{-1}), and a pindolol occupancy scan simulating a occupancy level of 50% (i.e., k$_3$ = 0.022 min^{-1}). Images were blurred as described above, measured time-activity curves were analyzed by kinetic modeling, and BP values were derived as the difference between the "distribution volumes" in the spheres and the background. Although measured BP decreased with decreasing sphere size, measured occupancy was within 0.1% of true occupancy for all spheres (measured occupancy was 50.1% for the largest sphere and 49.9% for the smallest sphere). These simulations confirm the theoretical analysis presented in appendix and support the hypothesis that the partial volume effect does not explain the relatively greater pindolol-induced decrease in DRN BP compared to corticolimbic regions.

ROI Identification. Since DRN boundaries are not identifiable on the MRI, the boundaries for the DRN ROI were drawn directly on the PET scan around the activity identified as the DRN. The size and shape of this region was kept constant for each subject, but the placement was varied slightly from one scan to the other to compensate for small errors in PET to MRI coregistration. Since DRN activity concentrations were more visible on scan 1 than scans 2, 3, and 4 (see Figure 2), it is plausible that DRN region boundaries placements were more accurate for scan 1, yielding an underestimation of DRN BP on scans 2, 3, and 4. Since this problem was not encountered for the other regions, it could contribute to an apparent greater occupancy by pindolol in the DRN compared to the other regions.

To test this hypothesis, two additional analyses were completed. In the first one, the ROI was drawn on scan 1, and then directly applied on scan 2 to 4 without any correction. In the second analysis, the ROI was drawn on scan 2, and directly applied on scan 1, 3, and 4, again without correction. These two analyses addressed the possible bias due to lower visual identifiability of DRN in scans 2, 3, and 4 relative to scan 1, yet introduced another bias, in that a small error in PET to MRI coregistration would not affect the primary scan on which the region placement was based, but would affect the DRN measurement in the three other scans. The estimation of pindolol occupancy in the DRN was similar with the

Table 9. Pharmacodynamic Modeling of 5-HT$_{1A}$ Receptor Occupancy by Pindolol in DRN and Postsynaptic Regions

Region Parameter	Unconstrained Fit			Constrained Fit		
	E$_{max}$ Occupancy (%)	EC$_{50}$ Occupancy (ng mL^{-1})	r	E$_{max}$ Occupancy (%)	EC$_{50}$ Occupancy (ng mL^{-1})	r
DRN	95 ± 23	24 ± 15	0.68	100	27 ± 6	0.68
All other regions	53 ± 17	21 ± 18	0.50	100	80 ± 16	0.38

Values are parameter estimates and their standard error obtained by fitting an hyperbolic function Occ = E$_{max}$P/(EC$_{50}$ + P) to data from scans 2 and 4, where P is pindolol concentration (ng mL^{-1}) and Occ is receptor occupancy (%).

three methods (data not shown). Since each method has a potential (but different) bias, this suggests that the larger occupancy measured in the DRN is unlikely to result from a systematic misplacement of the ROI in scans 2, 3, and 4 relative to scan 1.

Nonspecific Binding.   Between region differences in nonspecific binding is another possible source of bias. Displacement studies performed in primates indicate that the nonspecific binding of [^{11}C]WAY 100635 is relatively uniform across brain regions (Farde et al. 1997) and equal to the cerebellum distribution volume, but nonspecific binding of [^{11}C]WAY 100635 has not been directly measured in humans. Therefore, it cannot be excluded that the nonspecific binding of [^{11}C]WAY 100635 is higher in cortical and limbic regions compared to the DRN. Such a difference would result in underestimation of the pindolol occupancy in cortical and limbic regions. However, the difference in nonspecific binding between the postsynaptic and DRN regions would have to be extremely large to account for the differences in pindolol occupancy observed in this study. For example, if the medial temporal lobe V_2 was 1.5 fold higher than the cerebellum V_T, the true decrease in medial temporal lobe BP from scan 1 to scan 2 would be 20% instead of 19%. Thus, while this factor might in theory bias the results, its impact is practically negligible.

Effect of Endogenous 5-HT.   Finally, we must discuss the possibility that pindolol administration might be associated with a larger increase of endogenous 5-HT in the DRN compared to corticolimbic regions and that endogenous 5-HT might effectively compete with [^{11}C]WAY 100635 for binding to 5-HT$_{1A}$ receptors. Under this scenario, the occupancy of 5-HT$_{1A}$ receptors by pindolol would be overestimated, and more so in the DRN that in the corticolimbic regions. However, we previously showed that, in baboons, administration of the 5-HT releaser fenfluramine failed to decrease [^{11}C]WAY 100635 specific binding (Parsey et al. 1999). Therefore, this mechanism is unlikely to explain the greater potency of pindolol to displace [^{11}C]WAY 100635 binding in the DRN compared to corticolimbic regions.

In conclusion, we failed to identify factors that would account for an artifactual result. The next question is whether this result is consistent with previously reported studies comparing the potency or affinity of pindolol between somatodendritic 5-HT$_{1A}$ autoreceptors and postsynaptic 5-HT$_{1A}$ receptors.

Pindolol Potency at Somatodendritic Autoreceptors and Postsynaptic Heteroreceptors

Some, but not all, preclinical studies provided direct evidence of a higher potency of pindolol at the 5-HT$_{1A}$ autoreceptors compared to postsynaptic 5-HT$_{1A}$ receptors. Romero et al. (1996) demonstrated that although pin-

dolol blocked the SSRI and LSD induced activation of 5-HT$_{1A}$ autoreceptors in the DRN, the same dose of pindolol failed to prevent 5-HT$_{1A}$ agonist induced inhibition of pyramidal cell firing in the hippocampus. On the other hand, Corradetti et al. (1998) reported similar potency of pindolol to block in vitro 5-HT$_{1A}$ activation in the DRN and the hippocampus.

Data from autoradiographic binding studies are contradictory. One in vitro autoradiographic study in rats, guinea-pigs, monkeys and humans showed similar potency of (−)pindolol to displace [^{3}H]WAY 100635 in DRN and hippocampus in the four species (Raurich et al. 1999). In humans, (−)pindolol K_I was 17.0 ± 5.9 nM (mean ± SEM, $n = 4$) and 17.3 ± 3.7 nM in DRN and hippocampus (CA1), respectively. However, using the same ligand ([^{11}C]WAY 100635), same general assay conditions, and the same number of human subjects ($n = 4$), Castro et al. (1999) reported significantly higher affinity of pindolol for 5-HT$_{1A}$ in the DRN (8.9 ± 1.1 nM) compared to the hippocampus (14.4 ± 1.5 nM in CA1, $p < .05$). The reason for this discrepancy is unclear, and additional studies are required to resolve this issue. In addition, binding parameters measured in vitro might not always provide an accurate estimate of in vivo binding parameters since in vitro assays are performed under nonphysiological temperature and buffer conditions (Laruelle et al. 1994a).

Two studies have reported in vivo inhibition studies of WAY 100635 binding by pindolol in rodents. Corradetti et al. (1998) reported blocking studies of in vivo [^{3}H]WAY 100635 binding by (−)pindolol (15 mg kg^{-1}, i.p.) and showed almost complete and equivalent binding inhibition in the DRN (−76%), CA1 (-69%), CA3 (−79%) and parietal cortex (−82%). On the other hand, Hirani et al. (2000) reported inhibition of [^{11}C]WAY 100635 binding in rats studied with a small animal PET scanner by various doses of (−)pindolol (ranging from 0.001 to 3 mg kg^{-1}, i.v.). The ED$_{50}$ of (−)pindolol for inhibiting [^{11}C]WAY 100635 binding was significantly lower in the DRN (ED$_{50}$ = 0.26 ± 0.05 mg kg^{-1}) compared to the hippocampus (0.48 ± 0.12 mg kg^{-1}) and the frontal cortex (0.44 ± 0.13 mg kg^{-1}).

Previous studies of (±)pindolol occupancy in humans with PET are also inconclusive. Andree et al. (1999) studied inhibition of [^{11}C]WAY 100635 binding in three male volunteers, 2 h following oral administration of 10 mg of pindolol. PET data were acquired for 69 min and analyzed with the peak equilibrium method (Farde et al. 1998). Pindolol occupancy of 5-HT$_{1A}$ receptors in the DRN was 16 ± 9% and was not significantly different from the occupancy in temporal and frontal cortices (24 ± 5%). Rabiner et al. (2000) reported occupancy of 5-HT$_{1A}$ receptors by pindolol two hours following oral administration of 5 mg ($n = 3$), 10 mg ($n = 4$), and 20 mg ($n = 3$) of pindolol. PET data were acquired for 90 min and analyzed with the basis function

implementation of the simplified reference tissue model (Gunn et al. 1998). Following the 5-mg dose, no significant occupancy was detected. Following the 10-mg dose, a significantly larger occupancy was detected in the DRN (37 ± 9%) compared to the cortical regions (13 ± 8%, $p < .001$). Following the 20-mg dose, the DRN occupancy (39 ± 3%) was similar to the cortical occupancy (46 ± 10%, $p = .24$).

Results of these PET studies are not directly comparable to the results reported here. We measured occupancy following sustained administration of a controlled release formulation of pindolol, rather than following single dose administration of pindolol. Duration of scan was 69 min, 90 min, and 100 min in Andree et al. (1999), Rabiner et al. (2000) and this study, respectively. Data were analyzed with peak equilibrium method (Andree et al. 1999), simplified reference tissue model (Rabiner et al. 2000), and full kinetic analysis using the arterial plasma as input function (this study). Outcome measures derived from the scan data were BP normalized to the cerebellum (V_3'') in Andree et al. (1999) and Rabiner et al. (2000), and absolute BP here. While all studies analyzed the DRN, postsynaptic occupancy was derived from the analysis of 2, 14, and 10 regions in Andree et al. (1999), Rabiner et al. (2000), and this study, respectively. However, none of these factors are a priori suspected to bias the comparison of the DRN versus cortical occupancy. For example, we also computed the occupancies based on V_3'' and obtained similar results to those obtained with BP (Table 6).

The inconsistent results reported in prior studies might be due to the small number of subjects studied (3 to 4). We calculated the effect size (dt) detected in this study as dt = $(\mu_1 - \mu_2)/SD$, were μ is the mean regional occupancy (DRN vs. corticolimbic). Assuming that the true effect size is approximated by the effect size observed in this study (dt = 1.37), the number of subjects required to detect a significant difference in DRN vs. corticolimbic occupancy with a power of 0.80 (using a two-tailed test and a significance level of 0.05) is 10. With the number of subjects studied here ($n = 8$), the power was 0.70 for each dose. With the number of subjects reported by Andree et al. (1999) and Rabiner et al. (2000) (less than five subjects per dose), the power was less than 0.5, i.e., these studies were more likely not to detect a significant difference than to detect one.

Possible Mechanism Underlying Pindolol DRN Selectivity

If we accept that occupancy of pindolol is higher in the DRN compared to corticolimbic regions, we must consider potential mechanisms underlying these regional differences. We will speculate here about the potential involvement of regional differences in receptor coupling to G-proteins and degree of receptor internalization.

Receptor Coupling to G-proteins. Pre- and post-synaptic 5-HT$_{1A}$ receptors exhibit well characterized pharmacological differences. In general, pre-synaptic receptors are more "agonist" sensitive compared to post synaptic receptors (Meller et al. 1990; Jolas et al. 1995). A number of drugs act as full agonists in the DRN but as partial agonists in the hippocampus (such as buspirone or ipsapirone); or as partial agonists in the DRN and as antagonists in the hippocampus (such as NAN-190 and BMY 7378) (Andrade and Nicoll 1987; Sprouse and Aghajanian 1987; Sinton and Fallon 1988; Sprouse and Aghajanian 1988; Hjorth and Sharp 1990; Greuel and Glaser 1992; Fabre et al. 1997). Importantly, these pharmacological differences are detected in functional assays in vivo, rather than in binding studies. The binding properties of these compounds to the pre- and post-synaptic receptors, as assessed in vitro, are generally similar (Radja et al. 1992). Thus, the different pharmacology of 5-HT$_{1A}$ receptors across regions does not involve differences in binding sites, but rather efficacy of coupling with signal transduction system which might only be present in vivo.

Recent preclinical studies show that pindolol is a weak agonist at the pre-synaptic receptors, since pindolol by itself reduces the firing rate of DRN 5-HT neurons, an effect antagonized by WAY 100635 (Clifford et al. 1998; Haddjeri et al. 1999). In cells transfected with the human 5-HT$_{1A}$ receptor, pindolol induces an increase in [^{35}S]GTPγS binding, a prototypical agonist response (Newman-Tancredi et al. 1998). However, the agonist activity of pindolol is markedly lower than that of 5-HT (stimulation of [^{35}S]GTPγS by pindolol is only 20% of the activation by 5-HT). Therefore, in the presence of increased 5-HT concentration, as induced by SSRI, pindolol acts as an antagonist, preventing the inhibition of cell firing and the decrease in 5-HT release (Hjorth 1996; Romero et al. 1996; Gobert and Millan 1999). The agonist nature of the interaction of pindolol with 5-HT$_{1A}$ receptors might account for the regional differences in binding observed in this study.

Like all G-protein linked receptors, the binding of agonists to 5-HT$_{1A}$ is modulated by the coupling of the receptors to G-proteins (Hall et al. 1986; Emerit et al. 1990; Watson et al. 1999), whereas the binding of pure antagonists, such as [^{3}H]WAY 100365 is unaffected (Gozlan et al. 1995). In fact, the number of sites labeled by [^{3}H]8-OH-DPAT in corticolimbic areas is 50% lower than the number of sites labeled with [^{3}H]WAY 100635 (Gozlan et al. 1995), supporting the hypothesis that only about 50% of 5-HT$_{1A}$ receptors are configured in agonist high affinity state in these regions. When fitting our data to a simple competition model, we found that, in the concentration range used in this study, the maximal number of pindolol binding sites corresponded to about 50% of sites labeled by [^{11}C]WAY 100635 in cortical and limbic areas, whereas it corresponded to 95% of

sites labeled by [^{11}C]WAY 100635 in the DRN (Table 9). Therefore, it is conceivable that, in vivo, most of the DRN sites would be configured in the agonist high affinity state, compared to only 50% of the sites in corticolimbic areas.

Internalization. Another possible mechanism that could account for regional differences in the in vivo affinity of pindolol for 5-HT$_{1A}$ receptors would be regional differences in the degree of internalization of 5-HT$_{1A}$ receptors (Riad et al. 1999; Rudell et al. 1999). [^{11}C]WAY 100635 and pindolol, being lipophilic, would be expected to bind to both internalized and externalized receptors. The cellular localization of receptors affects the apparent affinity of some radioligands, due to ligand trapping in endosomal compartment and differences in receptor microenvironment (for review and references, see Laruelle 2000). If pindolol displays higher affinity for internalized versus externalized receptors, and if a larger proportion of 5-HT$_{1A}$ receptors are internalized in the DRN compared to the corticolimbic areas, then the apparent in vivo affinity of pindolol would be higher in the DRN compared to the postsynaptic areas. In this regard, it is interesting to note that the occupancy of DRN by pindolol was equivalent at scan 2 (40%) and 3 (38%, i.e., decrease of 5% in occupancy), whereas occupancy of other regions by pindolol decreased from scan 2 (18%) to scan 3 (12%, i.e., decrease of 33%). This observation is consistent with a slower effective dissociation rate of pindolol in DRN compared to other regions, possibly due to intracellular trapping mechanisms (Chugani et al. 1988; Laruelle 2000).

It should be stressed that both mechanisms discussed here (regional differences in G-protein coupling and degree of internalization) might apply only to the in vivo situation, given that in vitro preparations might disrupt coupling and the subcellular distribution of receptors. Both mechanisms should only be viewed as working hypotheses to be further evaluated.

Clinical Implications

The results of this study suggest that, at doses used in clinical studies of pindolol to augment SSRI treatment (2.5 mg, t.i.d.), the occupancy of 5-HT$_{1A}$ is moderate and highly variable between subjects and this factor may explain the variable results obtained in clinical studies.

Estimation of Occupancy Achieved in Clinical Trials. To our knowledge, only one clinical study reported plasma levels of pindolol. Perez et al. (1999) measured pindolol plasma levels of 9.9 ± 5.1 (SD) ng mL^{-1} in a sample of 40 subjects treated with a combination of pindolol (2.5 mg, t.i.d.) and SSRI's (fluoxetine, paroxetine, fluvoxamine, or clomipramine). Plasma levels were obtained 10 days after initiation of pindolol augmentation, but the temporal relationship between sampling and dosing was not reported. Assuming that 9.9 ng mL^1 corresponds to C$_{av}$, our data (using parameters from Table 9) would indicate a rather low 5-HT$_{1A}$ occupancy (28% and 17% in the DRN and corticolimbic regions, respectively).

This conclusion is at variance with results from Raurich et al. (1999) who concluded that, at doses of 2.5 mg, t.i.d., pindolol plasma levels should be high enough to induce more than 50% occupancy of 5-HT$_{1A}$ receptors. This conclusion was based on the following calculation. Given a pindolol molecular weight of 248, a plasma concentration of 9.9 ng mL^{-1} corresponds to 39 nM. Assuming similar pharmacokinetic parameters for both (+) and (−)pindolol, the concentration of the active enantiomer (−)pindolol would be 19.5 nM, which is higher than the in vitro K$_I$ of pindolol for [^{11}C]WAY 100635 binding in human DRN (17 nM) reported by these authors. The difference between the conclusion of Raurich et al. (1999) and the conclusion of this study stems from two factors. First, Raurich et al. (1999) did not take into account the binding of pindolol to plasma proteins. The plasma free fraction (i.e., not bound to plasma proteins) of pindolol has been reported as approximately 70% (Lima et al. 1986), 60% (Meier 1982), or 40% (Belpaire et al. 1982) in healthy volunteers.

Experimental evidence has demonstrated that for drugs that crosses the blood brain barrier by passive diffusion, the intracerebral free concentration equilibrates with the free plasma concentration (Kawai et al. 1991; Laruelle et al. 1994a). Thus, a total (bound to plasma proteins and free) pindolol plasma concentration of 19.5 nM would correspond to a free pindolol concentration of 10.7 nM (assuming a free fraction of 55%). Given a K$_I$ of 17 nM, the occupancy achieved in clinical studies would be 39%. The second factor is that the affinity of pindolol for DRN receptors might be overestimated in vitro, to the extent that assay conditions (temperature, buffer) are selected to optimize binding. Our data indicate a EC$_{50}$ of (±)pindolol in the DRN of 24 ng mL^{-1}, which corresponds to 97 nM of (±)pindolol, 48 nM of (−)pindolol, and 27 nM of free (−)pindolol. Thus, the PET data indicate an in vivo K$_I$ of pindolol of 27 nM. Given a K$_I$ of 27 nM, the occupancy achieved in clinical studies would be only 28%, assuming that the pindolol plasma values reported by Perez et al. (1999) are representative.

It is unclear if 28% occupancy of DRN 5-HT$_{1A}$ receptors is enough to achieve the desired clinical effect. The minimal occupancy of DRN 5-HT$_{1A}$ receptors needed to achieve blockade of the SSRI induced activation of these receptors has not been well documented. In the classic study of Romero et al. (1996), a (−)pindolol dose of at least 10 mg/kg i.p. was required to significantly block the decrease in striatal 5-HT extracellular concentration induced by direct application of citalopram (50 μM) in the DRN. To our knowledge, the occupancy of

DRN 5-HT$_{1A}$ receptors achieved by 10 mg/kg i.p. pindolol in the rat has not been reported. Yet, a dose of 15 mg/kg, i.p. (−)pindolol has been reported to occupy 76% of DRN 5-HT$_{1A}$ receptors (Corradetti et al. 1998) and it is likely that the occupancy following 10 mg/kg, i.p. is in the range of 50%, i.e., higher than the 28% achieved in clinical studies. Studies combining occupancy and electrophysiological or microdialysis measurements are needed to clarify this question.

Our data indicate that a pindolol regimen of 6.25 mg, t.i.d. (18.75 mg/day) would be necessary to achieve 50% occupancy of DRN 5-HT$_{1A}$ receptors. This regimen (6.25 mg, t.i.d.) would be 2.5 times higher than currently used regimen (2.5 mg, t.i.d.). While this dosage would still be in the lower range of doses used for the management of high blood pressure (30–45 mg/day), it is likely to be associated with more pronounced side effects, due to significant β-adrenergic receptor blockade, and might be impractical in routine outpatient clinical care. In addition, pharmacokinetic interactions between antidepressants and beta adrenergic blockers must be carefully considered (Ferrari et al. 1991). Finally, it should be kept in mind that the present study was performed in males, to avoid potential confounding effects of menstrual cycle on occupancy measurement. Since estrogens affect 5-HT$_{1A}$ receptor function differently in the DRN and corticolimbic regions (Clarke and Goldfarb 1989; Clarke et al. 1996), it will be important to replicate this study in females.

Between Subject Variability. The second practical implication of this study is the large between subject variability in both pindolol plasma levels and occupancy, particularly at the lower dose (Table 5). This variability might also account for the variability in the effect observed in clinical studies. Such a variability suggests that blood level monitoring might be useful in clinical studies to adjust the dose to levels compatible with appropriate occupancy.

To evaluate the feasibility of such an approach, we evaluated the relationship between pindolol plasma levels and regional occupancy. In the DRN, a significant linear relationship was found between 5-HT$_{1A}$ occupancy and pindolol plasma level at scan 3 ($r^2 = 0.49$, $p = .05$) and scan 4 ($r^2 = 0.65$, $p = .001$), but not at scan 2 ($r^2 = 0.20$, $p = .25$). The fact that plasma pindolol levels explained only 20 to 60% of the variability of DRN occupancy (within a given condition) is expected: both measures are associated with noise (particularly the DRN), and this relationship does not take into account possible between subject differences in pindolol plasma free fraction. Thus, despite these limitations, measurements of plasma levels would be useful for monitoring occupancy of 5-HT$_{1A}$ receptors in the DRN. On the other hand, a surprising finding was the quasi-absence of relationship between plasma levels and the average occu-

pancy in corticolimbic regions: scan 2: $r^2 = 0.14$, $p = .34$; scan 3: $r^2 = 0.04$, $p = .63$; scan 4: $r^2 = 0.02$, $p = .68$. We would have predicted the opposite observation (i.e., a better relationship between plasma values and corticolimbic occupancy than with DRN occupancy) because DRN [^{11}C]WAY 100635 BP measurement is associated with more noise than cortico-limbic [^{11}C]WAY 100635 BP measurements. Each of the ten corticolimbic regions are significantly larger than the DRN and provide a more reliable measurement of [^{11}C]WAY 100635 BP (Parsey et al. 2000). Therefore, we must conclude that, at a given pindolol plasma level, there is a greater between subject variability in the corticolimbic 5-HT$_{1A}$ receptor occupancy compared to DRN 5-HT$_{1A}$ receptor occupancy.

This observation is, in fact, consistent with the pharmacodynamic analysis presented in Table 9. The unconstrained analysis suggested that pindolol labels with high affinity (EC$_{50}$ of 24 ng mL^{-1}) one population of sites in the DRN, while it labels only about 50% of corticolimbic 5-HT$_{1A}$ receptors with high affinity (EC$_{50}$ = 21 ng mL^{-1}). Thus, in corticolimbic regions, 5HT$_{1A}$ receptors might be configured in states of high and low affinity for pindolol with the low affinity sites not being occupied by pindolol in the dose range used in this study. The large between subject variability in corticolimbic occupancy suggests a significant between subject variability in the proportion of high versus low affinity sites in these regions. Conversely, the data suggest low between subject variability in the EC$_{50}$ for the high affinity sites, since DRN occupancy is reasonably predicted by pindolol plasma levels.

Therapeutic Window. The selective occupancy of pindolol observed in this study suggests the existence of a therapeutic window for pindolol plasma concentrations. The therapeutic window includes the range of pindolol concentrations at which a marked difference is reached between DRN occupancy (which should be high in order to potentiate SSRI effects on 5-HT transmission) and cortical occupancy (which should be low in order to maintain activation of postsynaptic 5-HT$_{1A}$ receptors). This window is illustrated in Figure 6, which simulates inhibition of [^{11}C]WAY 100635 binding as a function of plasma levels of (±)pindolol. The following parameters were used in this simulation: the DRN includes one population of sites which binds pindolol with an EC$_{50}$ of 24 ng mL^{-1}; the cortex includes two populations of sites, each corresponding to 50% of the total [^{11}C]WAY 100635 binding sites; cortical high affinity sites have the same affinity as the DRN sites (24 ng mL^{-1}); cortical low affinity sites have an affinity of 140 ng mL^{-1}, so that the average affinity of the cortical sites is 82 ng mL^{-1}. The triangles represent the differences in occupancy between DRN and cortical regions. This simulation shows that plasma level associated with 50%
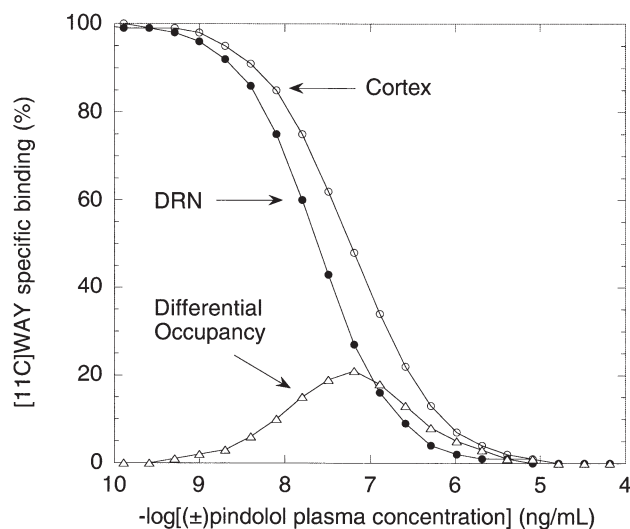
Figure 6. Simulation of [^{11}C]WAY 100635 displacement by pindolol as a function of (±)pindolol plasma concentration in DRN (closed circles) and cortical (open circles) regions, based on the following model parameters: the DRN includes one population of sites that bind pindolol with an EC$_{50}$ of 24 ng mL^{-}1; the cortex includes two population of sites, each corresponding to 50% of the total [^{11}C]WAY 100635 binding sites; cortical high affinity sites have the same affinity as the DRN sites (24 ng mL^{-1}); cortical low affinity sites have an affinity of 140 ng mL^{-1}, so that the average affinity of the cortical sites is 82 ng mL^{-1}. The triangles represent the differences in occupancy between DRN and cortical regions, which is maximal in the 32 to 128 ng mL^{-1} plasma range.

occupancy of DRN 5-HT$_{1A}$ receptors is associated with a 18% occupancy difference between DRN and cortical regions. This difference is close to the maximal difference, suggesting that this level of DRN occupancy would be an appropriate target.

Profile of the Ideal Compound for Augmentation of SSRI Antidepressant Effects. Assuming that selective blockade of 5HT$_{1A}$ autoreceptors is useful for hastening clinical response to SSRIs, the PET data presented here provide some clues about the desired properties of compounds selected for this application. The data suggest that pindolol might not be the ideal compound, since the side effects associated with its beta-adrenergic blocking properties might preclude its use in routine clinical practice at doses (15–25 mg/day) required to block 50% of the DRN 5-HT$_{1A}$ receptors.

It is currently assumed that silent 5-HT$_{1A}$ antagonists would be the optimal pharmacological agents for this application: WAY 100635 or other silent antagonists provide superior potentiation of he acute effects of SSRIs on 5-HT transmission compared to pindolol, a difference attributed to the fact that pindolol is a partial agonist (Sharp et al. 1993; Clifford et al. 1998; Gartside

et al. 1999). However, if DRN selectivity is a unique feature of partial agonists, a weak and DRN selective partial agonist might still be the drug of choice for this application. On the other hand, if DRN selectivity is due to regional differences in the proportion of high and low affinity sites for agonists, this property might not be important, to the extend that 5-HT acts primarily, if not exclusively, on receptors configured in high agonist affinity state. PET studies of other 5HT$_{1A}$ partial agonists, silent antagonists and agonists are warranted to evaluate the relationship between pharmacological profile and DRN selectivity. Finally, given that the goal of this pharmacological strategy is to hasten therapeutic response, appropriate plasma levels of the candidate drug should be reached rapidly, maybe using an initial loading dose. Again, PET imaging provides a unique tool to define the relationship between pharmacokinetic and therapeutic windows.

CONCLUSIONS

This study evaluated the occupancy of 5-HT$_{1A}$ receptor achieved during treatment with pindolol in humans. The results indicate that pindolol significantly decreased [^{11}C]WAY 100635 BP at all doses tested. Based on these data, the occupancy of DRN 5-HT$_{1A}$ receptors achieved during clinical trials aimed at hastening or augmenting the antidepressant effects of SSRIs was estimated to be in the order of 30%, which might be less than optimal for achieving the desired potentiation of 5-HT transmission. This factor, as well as the important between subject variability in occupancy, might account for the mixed results reported in double blind, placebo controlled studies. However, pindolol demonstrated significant in vivo selectivity for DRN 5-HT$_{1A}$ autoreceptors relative to corticolimbic postsynaptic receptors. This DRN selectivity is desirable for potentiation of 5-HT transmission, and represents an important proof of concept for the development of new 5-HT$_{1A}$ agents for this application. Early evaluation of new drugs with PET imaging will enable rapid screening of compounds based on DRN selectivity, and more rigorous determination of doses to be tested in clinical trials.

ACKNOWLEDGMENTS

REFERENCES

Abi-Dargham A, Laruelle M, Seibyl J, Rattner Z, Baldwin RM, Zoghbi SS, Zea-Ponce Y, Bremner JD, Hyde TM, Charney DS, Hoffer PB, Innis RB (1994): SPECT measurement of benzodiazepine receptors in human brain with [^{123}I]iomazenil: Kinetic and equilibrium paradigms. J Nucl Med 35:228–238

Abi-Dargham A, Martinez D, Mawlawi O, Simpson N, Hwang DR, Slifstein M, Anjilvel S, Pidcock J, Guo NN, Lombardo I, Mann JJ, Van Heertum R, Foged C, Halldin C, Laruelle M (2000): Measurement of striatal and extrastriatal dopamine D1 receptor binding potential with [^{11}C]NNC 112 in humans: Validation and reproducibility. J Cereb Blood Flow Metab 20:225–243

Aellig WH, Nuesch E, Pacha W (1982): Pharmacokinetic comparison of pindolol 30 mg retard and 15 mg normal tablets. Eur J Clin Pharmacol 21:451–455

Andrade R, Nicoll RA (1987): Novel anxiolytics discriminate between postsynaptic serotonin receptors mediating different physiological responses on single neurons of the rat hippocampus. Naunyn Schmiedebergs Arch Pharmacol 336:5–10

Andree B, Thorberg SO, Halldin C, Farde L (1999): Pindolol binding to 5-HT1A receptors in the human brain confirmed with positron emission tomography. Psychopharmacology (Berl) 144:303–305

Artigas F, Perez V, Alvarez E (1994): Pindolol induces a rapid improvement of depressed patients treated with serotonin reuptake inhibitors. Arch Gen Psychiatry 51:248–251

Artigas F, Romero L, de Montigny C, Blier P (1996): Acceleration of the effect of selected antidepressant drugs in major depression by 5-HT1A antagonists. Trends Neurosci 19:378–83

Bakish D, Hooper CL, Thornton MD, Wiens A, Miller CA, Thibaudeau CA (1997): Fast onset: An open study of the treatment of major depressive disorder with nefazodone and pindolol combination therapy. Int Clin Psychopharmacol 12:91–97

Bel N, Artigas F (1992): Fluvoxamine preferentially increases extracellular 5-hydroxytryptamine in the raphe nuclei: An in vivo microdialysis study. Eur J Pharmacol 229:101–103

Belpaire FM, Bogaert MG, Rosseneu M (1982): Binding of beta-adrenoceptor blocking drugs to human serum albumin, to alpha 1-acid glycoprotein and to human serum. Eur J Clin Pharmacol 22:253–256

Berman RM, Anand A, Cappiello A, Miller HL, Hu XS, Oren DA, Charney DS (1999): The use of pindolol with fluoxetine in the treatment of major depression: Final results from a double-blind, placebo-controlled trial. Biol Psychiatry 45:1170–1177

Berman RM, Darnell AM, Miller HL, Anand A, Charney DS (1997): Effect of pindolol in hastening response to fluoxetine in the treatment of major depression: A double-blind, placebo-controlled trial. Am J Psychiatry 154:37–43

Blier P, Bergeron R (1995): Effectiveness of pindolol with selected antidepressant drugs in the treatment of major depression. J Clin Psychopharmacol 15:217–222

Blier P, de Montigny C (1985): Serotoninergic but not noradrenergic neurons in rat central nervous system adapt to long-term treatment with monoamine oxidase inhibitors. Neuroscience 16:949–955

Blier P, de Montigny C (1994): Current advances and trends in the treatment of depression. Trends Pharmacol Sci 15:220–226

Borchard U (1990): Pharmacokinetics of beta-adrenoceptor blocking agents: Clinical significance of hepatic and/or renal clearance. Clin Physiol Biochem 8:28–34

Bordet R, Thomas P, Dupuis B (1998): Effect of pindolol on onset of action of paroxetine in the treatment of major depression: Intermediate analysis of a double-blind, placebo- controlled trial. Reseau de Recherche et d'Experimentation Psychopharmacologique. Am J Psychiatry 155:1346–1351

Carson RE (1986): Parameters estimation in positron emission tomography. In Phelps ME, Mazziotta JC, Schelbert HR (eds), Positron Emission Tomography. Principles and Applications for the Brain and the Heart. New York, Raven Press, pp 347–390

Castro ME, Harrison PJ, Pazos, Sharp T (2000): Affinity of (±)-pindolol, (−)-penbutolol, and (−)-tertatolol for pre- and postsynaptic serotonin 5-HT(1A) receptors in human and rat brain. J Neurochem 75(2):755–762

Chaput Y, de Montigny C, Blier P (1986): Effects of a selective 5-HT reuptake blocker, citalopram, on the sensitivity of 5-HT autoreceptors: Electrophysiological studies in the rat brain. Naunyn Schmiedebergs Arch Pharmacol 333:342–348

Chugani DC, Ackermann RF, Phelps ME (1988): In vivo [^{3}H]spiperone binding: Evidence for accumulation in corpus striatum by agonist-mediated receptor internalization. J Cereb Blood Flow Metab 8:291–303

Clarke WP, Goldfarb J (1989): Estrogen enhances a 5-HT1A response in hippocampal slices from female rats. Eur J Pharmacol 160:195–197

Clarke WP, Yocca FD, Maayani S (1996): Lack of 5-hydroxytrytamine1A-mediated inhibition of adenylyl cyclase activity in dorsal raphe male and female rats. J Pharmacol Exp Ther 277:1259–1266

Clifford EM, Gartside SE, Umbers V, Cowen PJ, Hajos M, Sharp T (1998): Electrophysiological and neurochemical evidence that pindolol has agonist properties at the 5-HT1A autoreceptor in vivo. Br J Pharmacol 124:206–212

Corradetti R, Laaris N, Hanoun N, Laporte AM, Le Poul E, Hamon M, Lanfumey L (1998): Antagonist properties of (−)-pindolol and WAY 100635 at somatodendritic and postsynaptic 5-HT1A receptors in the rat brain. Br J Pharmacol 123:449–462

Dillon KA, Gross-Isseroff R, Israeli M, Biegon A (1991): Autoradiographic analysis of serotonin 5-HT1A receptor binding in the human brain postmortem: Effects of age and alcohol. Brain Res. 554:56–64

Dreshfield LJ, Wong DT, Perry KW, Engleman EA (1996): Enhancement of fluoxetine-dependent increase of extracellular serotonin (5-HT) levels by (−)-pindolol, an antagonist at 5-HT1A receptors. Neurochem Res 21:557–562

Drevets W, Frank E, Price J, Kupfer D, Holt D, Greer PJ, Huang Y, Gautier C, Mathis C (1999): PET imaging of serotonin 1A receptor binding in depression. Biol Psychiatry 1375–1387

Duvernoy H (1991): The human brain. Surface, three-dimensional sectional anatomy and MRI. New York, Sringer-Verlag Wien

Emerit MB, el Mestikawy S, Gozlan H, Rouot B, Hamon M (1990): Physical evidence of the coupling of solubilized 5-HT1A binding sites with G regulatory proteins. Biochem Pharmacol 39:7–18

Fabre V, Boni C, Mocaer E, Lesourd M, Hamon M, Laporte AM (1997): [H-3]Alnespirone: A novel specific radioligand of 5-HT1A receptors in the rat brain. Eur J Pharmacol 337:297–308

Farde L, Ginovart N, Ito H, Lundkvist C, Pike VW, McCarron JA, Halldin C (1997): PET-characterization of [carbonyl-C-11]WAY-100635 binding to 5-HT1A receptors in the primate brain. Psychopharmacology 133:196–202

Farde L, Ito H, Swahn CG, Pike VW, Halldin C (1998): Quantitative analyses of carbonyl-carbon-11-WAY-100635 binding to central 5-hydroxytryptamine-1A receptors in man. J Nucl Med 39:1965–1971

Ferrari S, Leemann T, Dayer P (1991): The role of lipophilicity in the inhibition of polymorphic cytochrome P450IID6 oxidation by beta-blocking agents in vitro. Life Sci 48:2259–2265

Forster EA, Cliffe IA, Bill DJ, Dover GM, Jones D, Reilly Y, Fletcher A (1995): A pharmacological profile of the selective silent 5-HT1A receptor antagonist, WAY-100635. Eur J Pharmacol 281:81–88

Gandelman MS, Baldwin RM, Zoghbi SS, Zea-Ponce Y, Innis RB (1994): Evaluation of ultrafiltration for the free fraction determination of single photon emission computerized tomography (SPECT) radiotracers: β-CIT, IBF and iomazenil. J Pharmaceutical Sci 83:1014–1019

Gartside SE, Clifford EM, Cowen PJ, Sharp T (1999): Effects of (−)-tertatolol, (−)-penbutolol and (+/-)-pindolol in combination with paroxetine on presynaptic 5-HT function: An in vivo microdialysis and electrophysiological study. Br J Pharmacol 127:145–152

Gobert A, Millan MJ (1999): Modulation of dialysate levels of dopamine, noradrenaline, and serotonin (5-HT) in the frontal cortex of freely-moving rats by (−)- pindolol alone and in association with 5-HT reuptake inhibitors: Comparative roles of beta-adrenergic, 5-HT1A, and 5-HT1B receptors. Neuropsychopharmacology 21:268–284

Gozlan H, Thibault S, Laporte AM, Lima L, Hamon M (1995): The selective 5-HT1A antagonist radioligand [³H]WAY 100635 labels both G-protein-coupled and free 5-HT1A receptors in rat brain membranes. Eur J Pharmacol 288:173–186

Greuel JM, Glaser T (1992): The putative 5-HT1A receptor antagonists NAN-190 and BMY 7378 are partial agonists in the rat dorsal raphe nucleus in vitro. Eur J Pharmacol 211:211–219

Gunn RN, Sargent PA, Bench CJ, Rabiner EA, Osman S, Pike VW, Hume SP, Grasby PM, Lammertsma AA (1998): Tracer kinetic modeling of the 5-HT1A receptor ligand [carbonyl-¹¹C]WAY- 100635 for PET. Neuroimage 8:426–440

Haddjeri N, de Montigny C, Blier P (1999): Modulation of the firing activity of rat serotonin and noradrenaline neurons by (+/-)pindolol. Biol Psychiatry 45:1163–1169

Hall H, Lundkvist C, Halldin C, Farde L, Pike VW, McCarron JA, Fletcher A, Cliffe IA, Barf T, Wikstrom H, Sedvall G (1997): Autoradiographic localization of 5-HT1A receptors in the post-mortem human brain using [³H]WAY-100635 and [¹¹C]WAY-100635. Brain Res 745:96–108

Hall MD, Gozlan H, Emerit MB, el Mestikawy S, Pichat L, Hamon M (1986): Differentiation of pre- and post-synaptic high affinity serotonin receptor binding sites using physico-chemical parameters and modifying agents. Neurochem Res 11:891–912

Hirani E, Opacka-Juffry J, Gunn R, Khan I, Sharp T, Hume S (2000): Pindolol occupancy of 5HT(1A) receptors measured in vivo using small animal positron emission tomography with carbon-11 labelled WAY 100635. Synapse 36(4):330–341

Hjorth S (1996): (−)-Pindolol, but not buspirone, potentiates the citalopram-induced rise in extracellular 5-hydroxytryptamine. Eur J Pharmacol 303:183–186

Hjorth S, Sharp T (1990): Mixed agonist/antagonist properties of NAN-190 at 5-HT1A receptors: Behavioural and in vivo brain microdialysis studies. Life Sci 46:955–963

Hoyer D, Pazos A, Probst A, Palacios JM (1986): Serotonin receptors in the human brain. I. Characterization and autoradiographic localization of 5-HT1A recognition sites. Apparent absence of 5-HT1B recognition sites. Brain Res 376:85–96

Hoyer D, Schoeffter P (1991): 5-HT receptors: Subtypes and second messengers. J Recept Res 11:197–214

Hwang DR, Simpson N, Montoya J, Mann JJ, Laruelle M (1999): An improved one-pot procedure for the preparation of [¹¹C-carbonyl]WAY 100635. Nucl Med Biol 26:815–819

Invernizzi R, Belli S, Samanin R (1992): Citalopram's ability to increase the extracellular concentrations of serotonin in the dorsal raphe prevents the drug's effect in the frontal cortex. Brain Res 584:322–324

Jolas T, Schreiber R, Laporte AM, Chastanet M, De Vry J, Glaser T, Adrien J, Hamon M (1995): Are postsynaptic 5-HT1A receptors involved in the anxiolytic effects of 5-HT1A receptor agonists and in their inhibitory effects on the firing of serotonergic neurons in the rat? J Pharmacol Exp Ther 272:920–929

Kates WR, Abrams MT, Kaufmann WE, Breiter SN, Reiss AL (1997): Reliability and validity of MRI measurement of the amygdala and hippocampus in children with fragile X syndrome. Psychiatry Res Neuroimag 75:31–48

Kawai R, Carson RE, Dunn B, Newman AH, Rice KC, Blasberg RG (1991): Regional brain measurement of B$_{max}$ and K$_D$ with the opiate antagonist cyclofoxy: Equilibrium studies in the conscious rat. J Cereb Blood Flow Metab 11:529–544

Kessler RM, Ellis J Jr, Eden M (1984): Analysis of emission tomographic scan data: Limitations imposed by resolution and background. J Comput Assist Tomogr 8:514–522

Killiany RJ, Moss MB, Nicholson T, Jolez F, Sandor T (1997): An interactive procedure for extracting features of the brain from magnetic resonance images: The lobes. Human Brain Mapping 5:355:363

Laruelle M (2000): Imaging synaptic neurotransmission with in vivo binding competition techniques: A critical review. J Cereb Blood Flow Metab 20:423–451

Laruelle M, Abi-Dargham A, Al-Tikriti MS, Baldwin RM,

Zea-Ponce Y, Zoghbi SS, Charney DS, Hoffer PB, Innis RB (1994a): SPECT quantification of [123I]iomazenil binding to benzodiazepine receptors in nonhuman primates. II. Equilibrium analysis of constant infusion experiments and correlation with in vitro parameters. J Cereb Blood Flow Metab 14:453–465

Laruelle M, Baldwin RM, Rattner Z, Al-Tikriti MS, Zea-Ponce Y, Zoghbi SS, Charney DS, Price JC, Frost JJ, Hoffer PB, Innis RB (1994b): SPECT quantification of [123I]iomazenil binding to benzodiazepine receptors in nonhuman primates. I. Kinetic modeling of single bolus experiments. J Cereb Blood Flow Metab 14:439–452

Laruelle M, van Dyck C, Abi-Dargham A, Zea-Ponce Y, Zoghbi SS, Charney DS, Baldwin RM, Hoffer PB, Kung HF, Innis RB (1994c): Compartmental modeling of iodine-123-iodobenzofuran binding to dopamine D_2 receptors in healthy subjects. J Nucl Med 35:743–754

Levenberg K (1944): A method for the solution of certain problems in least squares. Quart Appl Math 2:164–168

Lima JJ, Binkley PF, Johnson J, Leier CV (1986): Dose- and time-dependent binding and kinetics of pindolol in patients with congestive heart failure. J Clin Pharmacol 26:253–257

Maes M, Libbrecht I, van Hunsel F, Campens D, Meltzer HY (1999): Pindolol and mianserin augment the antidepressant activity of fluoxetine in hospitalized major depressed patients, including those with treatment resistance. J Clin Psychopharmacol 19:177–182

Maes M, Vandoolaeghe E, Desnyder R (1996): Efficacy of treatment with trazodone in combination with pindolol or fluoxetine in major depression. J Affect Disord 41:201–210

Maione S, Palazzo E, Pallotta M, Leyva J, Berrino L, Rossi F (1997): Effects of imipramine on raphe nuclei and prefrontal cortex extracellular serotonin levels in the rat. Psychopharmacology (Berl) 134:401–405

Mawlawi OM, Weiss R, Shinn A, Pidcock J, Slifstien M, Laruelle M (1999): Performance characteristics of a head immobilization device for PET imaging. J Nucl Med 40:281P

Meier J (1982): Pharmacokinetic comparison of pindolol with other beta-adrenoceptor- blocking agents. Am Heart J 104:364–373

Meller E, Goldstein M, Bohmaker K (1990): Receptor reserve for 5-hydroxytryptamine1A-mediated inhibition of serotonin synthesis: Possible relationship to anxiolytic properties of 5-hydroxytryptamine1A agonists. Mol Pharmacol 37:231–237

Mintun MA, Raichle ME, Kilbourn MR, Wooten GF, Welch MJ (1984): A quantitative model for the in vivo assessment of drug binding sites with positron emission tomography. Ann Neurol 15:217–227

Newman-Tancredi A, Chaput C, Gavaudan S, Verriele L, Millan MJ (1998): Agonist and antagonist actions of (−)pindolol at recombinant, human serotonin1 (5-HT1A) receptors. Neuropsychopharmacology 18:395–398

Osman S, Lundkvist C, Pike VW, Halldin C, McCarron JA, Swahn CG, Ginovart N, Luthra SK, Bench CJ, Grasby PM, Wikstrom H, Barf T, Cliffe IA, Fletcher A, Farde L (1996): Characterization of the radioactive metabolites of the 5-HT1A receptor radioligand, [O-methyl-11C]WAY-100635, in monkey and human plasma by

HPLC: Comparison of the behavior of an identified radioactive metabolite with parent radioligand in monkey using PET. Nucl Med Biol 23:627–634

Parsey RV, Hwang DR, Simpson S, Guo N, Mawlawi O, Kegeles LS, Bergert B, Montoya J, Popilskis S, Mann JJ, Laruelle M (1999): PET studies of competition between [11C]carbonyl-WAY 100635 and endogenous serotonin. J Nucl Med 40:29P

Parsey RV, Slifstein M, Hwang DR, Abi-Dargham A, Simpson N, Mawlawi O, Guo N, Van Heertum R, Mann JJ, Laruelle M (2000): Validation and reproducibility of measurement of 5-HT1A receptors parameters with [carbonyl-11C]WAY-100635 in humans: Comparison of arterial and reference tissue input functions. J Cereb Blood Flow Metab 20:1111–1133

Perez V, Gilaberte I, Faries D, Alvarez E, Artigas F (1997): Randomised, double-blind, placebo-controlled trial of pindolol in combination with fluoxetine antidepressant treatment. Lancet 349:1594–1597

Perez V, Soler J, Puigdemont D, Alvarez E, Artigas F (1999): A double-blind, randomized, placebo-controlled trial of pindolol augmentation in depressive patients resistant to serotonin reuptake inhibitors. Grup de Recerca en Trastorns Afectius. Arch Gen Psychiatry 56:375–379

Pike VW, McCarron JA, Lammerstma AA, Osman S, Hume SP, Sargent PA, Bench CJ, Cliffe IA, Fletcher A, Grasby PM (1995): Exquisite delineation of 5-HT1A receptors in human brain with PET and [carbonyl-11C]WAY-100635. Eur J Pharmacol 301:R5–R7

Rabiner EA, Gunn RN, Castro ME, Sargent PA, Cowen PJ, Koepp MJ, Meyer JH, Bench CJ, Harrison PJ, Pazos A, Sharp T, Grasby PM (2000): Beta-blocker binding to human 5-HT(1A) receptors in vivo and in vitro: Implications for antidepressant therapy. Neuropsychopharmacology 23(3):285–93

Radja F, Daval G, Hamon M, Verge D (1992): Pharmacological and physicochemical properties of pre-versus postsynaptic 5-hydroxytryptamine1A receptor binding sites in the rat brain: A quantitative autoradiographic study. J Neurochem 58:1338–1346

Raurich A, Mengod G, Artigas F, Cortes R (1999): Displacement of the binding of 5-HT(1A) receptor ligands to pre- and postsynaptic receptors by (−)pindolol. A comparative study in rodent, primate and human brain. Synapse 34:68–76

Riad M, Doucer E, Hamon M, Descarries L (1999): 8-OH-DPAT internalizes 5HT1A autoreceptors in serotonin neurons of nucleus raphe dorsalis. Soc Neurosci Abstract 25:1466

Romero L, Bel N, Artigas F, de Montigny C, Blier P (1996): Effect of pindolol on the function of pre- and postsynaptic 5-HT1A receptors: In vivo microdialysis and electrophysiological studies in the rat brain. Neuropsychopharmacology 15:349–360

Rudell RG, Black JR, Shaw K (1999): Analysis of the mechanism of internalization of the human 5HT1A receptor. Soc Nuc Abstr 25:1467

Sargent PA, Kjaer KH, Bench CJ, Rabiner EA, Messa C, Meyer J, Gunn RN, Grasby PM, Cowen PJ (2000): Brain serotonin1A receptor binding measured by positron emission tomography with [11C]WAY-100635: Effects

of depression and antidepressant treatment. Arch Gen Psychiatry 57:174–180

Sharp T, McQuade R, Bramwell S, Hjorth S (1993): Effect of acute and repeated administration of 5-HT1A receptor agonists on 5-HT release in rat brain in vivo. Naunyn Schmiedebergs Arch Pharmacol 348:339–346

Sinton CM, Fallon SL (1988): Electrophysiological evidence for a functional differentiation between subtypes of the 5-HT1 receptor. Eur J Pharmacol 157:173–181

Sprouse JS, Aghajanian GK (1987): Electrophysiological responses of serotoninergic dorsal raphe neurons to 5-HT1A and 5-HT1B agonists. Synapse 1:3–9

Sprouse JS, Aghajanian GK (1988): Responses of hippocampal pyramidal cells to putative serotonin 5-HT1A and 5-HT1B agonists: A comparative study with dorsal raphe neurons. Neuropharmacology 27:707–715

Tada K, Kasamo K, Ueda N, Suzuki T, Kojima T, Ishikawa K (1999): Anxiolytic 5-hydroxytryptamine1A agonists suppress firing activity of dorsal hippocampus CA1 pyramidal neurons through a postsynaptic mechanism: Single-unit study in unanesthetized, unrestrained rats. J Pharmacol Exp Ther 288:843–848

Talairach J, Tournoux P (1988): Co-planar Stereotactic Atlas of the Human Brain. Three-Dimensional Proportional System: An Approach of Cerebral Imaging. New York, Theime Medical Publisher

Tome MB, Isaac MT, Harte R, Holland C (1997): Paroxetine and pindolol: A randomized trial of serotonergic autoreceptor blockade in the reduction of antidepressant latency. Int Clin Psychopharmacol 12:81–89

Watson J, Collin L, Ho M, Riley G, Scott C, Selkirk JV, Price GW (2000): 5HT(1A) receptor agonist antagonist binding affinity difference as a measure of intrinsic affinity in recombinant and native tissue systems. Br J Pharmacol 130(5):1108–1114

Woods RP, Cherry SR, Mazziotta JC (1992): Rapid automated algorithm for aligning and reslicing PET images. J Comp Assist Tomogr 16(4):620–633

Zanardi R, Artigas F, Franchini L, Sforzini L, Gasperini M, Smeraldi E, Perez J (1997): How long should pindolol be associated with paroxetine to improve the antidepressant response? J Clin Psychopharmacol 17:446–450

Zanardi R, Franchini L, Gasperini M, Lucca A, Smeraldi E, Perez J (1998): Faster onset of action of fluvoxamine in combination with pindolol in the treatment of delusional depression: A controlled study. J Clin Psychopharmacol 18:441–446

APPENDIX A

Partial Voluming and Occupancy Measurement

The formula for occupancy by a competitive ligand is

$$\frac{BP_{PRE} - BP_{POST}}{BP_{PRE}}$$

where BP_{PRE} and BP_{POST} are the binding potential of the radioligand before and after administration of the competitor, respectively. At equilibrium, BP is $A_T - A_{REF}$ where A_T and A_{REF} are true activities in the region of interest and region of reference, respectively ($A_T = BP + A_{REF}$). If the region of interest is isolated from all other regions with non-zero BP (i.e., separated by a distance of more than two FWHM of the point spread function of the scanner), the measured activity in the region of interest (A_M) will be a weighted average of the true activity in the region (A_T) and the surrounding background region (A_{REF}). This can be written as

$$A_M = \alpha A_T + (1 - \alpha)A_{REF}$$

with $0 \leq \alpha \leq 1$. The fact that the partial voluming coefficient α and the spill over coefficient $(1 - \alpha)$ must sum to 1 can be seen by letting $BP = 0$ so that the regional activity equals the background activity. In general, α varies directly with the volume of the region, i.e. tends toward 1 as the region volume grows larger. Letting 1 and 2 index pre- and post-competitor administration variables, the true activity levels are

$$A_{T_1} = BP_1 + A_{REF} \text{ and } A_{T_2} = BP_2 + A_{REF}$$

and the measured activities are

$$A_{M_1} = \alpha \cdot A_{T_1} + (1 - \alpha) \cdot A_{REF}$$

and

$$A_{M_2} = \alpha \cdot A_{T_2} + (1 - \alpha) \cdot A_{REF}$$

where it has been assumed that non-specific binding does not change from measurement 1 to measurement 2. The parameter α does not change because it is a function of the geometry of the region and of properties of the scanner but is independent of tracer concentrations.

The measured occupancy is computed as

$$\frac{(A_{M_1} - A_{REF}) - (A_{M_2} - A_{REF})}{A_{M_1} - A_{REF}} = \frac{A_{M_1} - A_{M_2}}{A_{M_1} - A_{REF}}$$

$$= \frac{(\alpha \cdot A_{T_1} + 1 - \alpha \cdot A_{REF}) - (\alpha \cdot A_{T_2} + (1 - \alpha) \cdot A_{REF})}{\alpha \cdot A_{T_1} + (1 - \alpha) \cdot A_{REF} - A_{REF}}$$

$$= \frac{\alpha(A_{T_1} - A_{T_2})}{\alpha(A_{T_1} - A_{REF})}$$

$$= \frac{(BP_1 + A_{REF}) - (BP_2 + A_{REF})}{BP_1 + A_{REF} - A_{REF}}$$

$$= \frac{BP_1 - BP_2}{BP_1}$$

$$= \text{true occupancy}$$

from which it can be seen that the measured occupancy is equivalent to true occupancy, independent of α and of partial volume effect.